The solution structure and self-association properties of the cyclic lipodepsipeptide pseudodesmin A support its pore forming potential

Davy Sinnaeve, Pieter M. S. Hendrickx, Johan Van hemel, Eric Peys, Bruno Kieffer and José C. Martins

D. Sinnaeve, P. M. S. Hendrickx, J. Van hemel, E. Peys, B. Kieffer and J. C. Martins (2009)
The solution structure and self-association properties of the cyclic lipodepsipeptide pseudodesmin A support its pore forming potential, Chem. Eur. J. 15, (46), 12653-12662, DOI: 10.1002/chem.200901885

CHEMISTRY
A EUROPEAN JOURNAL

FULL PAPER

DOI: 10.1002/chem.200((will be filled in by the editorial staff))

The solution structure and self-association properties of the cyclic lipodepsipeptide pseudodesmin A support its pore forming potential

Davy Sinnaeve,*[a] Pieter M. S. Hendrickx,[a] Johan Van hemel,[b] Eric Peys,[b] Bruno Kieffer[c] and José C. Martins*[a]

Abstract: Pseudodesmin A is a cyclic lipodepsipeptide (CLP) of the viscosin group with a moderate *in vitro* biological activity. For several CLPs, including members of this group, this activity has been related to the ability to form ion pores in cellular membranes. As their size does not allow individual CLPs to span the membrane bilayer, individual monomers must somehow assemble into a larger structure. Here, NMR has been used to demonstrate that in chloroform and other apolar organic solvents, pseudodesmin A monomers assemble into a supramolecular structure. These self-assembled structures can become sufficiently large to span the membrane bilayer as demonstrated with translational diffusion NMR measurements. With the aim to obtain more insight into the structural nature of this assembly, the solution conformation of pseudodesmin A was first determined using rOe restraints measured in acetonitrile, where no self-association occurs. The structure, which is found to be mostly similar to the previously described crystal structure, is shown to be retained within the supramolecular complex. Intermolecular rOe contacts obtained in chloroform together with chemical shift perturbation data provides structural insight into the organization of the self-associated complex. Based upon this analysis, a model for the organization of pseudodesmin A monomers in the supramolecular assembly is proposed, which is in agreement with the formation of bilayer spanning hydrophilic pores, providing the basis for a structure-function relationship for this type of CLPs. Finally, it is demonstrated that the differences previously reported between the crystal and solution conformation of WLIP, a close analogue of pseudodesmin A, are the result of the use of DMSO as solvent, whose strong hydrogen bonding capacity induces conformational exchange.

Keywords: cyclic lipodepsipeptide • WLIP • diffusion NMR • self-assembly • ion channels

Introduction

Cyclic lipodepsipeptides (CLPs)[1, 2] are small molecules that consist of an oligopeptide chain that is at least partially cyclised through a lactone (or depsi) bond between the C-terminus and a side chain alcohol group, while the N-terminus is coupled to a fatty acid moiety via an amide bond. These compounds are produced as secondary metabolites by several micro-organisms, including *Pseudomonas* bacteria, and mostly consist of uncommon or modified amino acids, such as D-amino acids. Pseudodesmin A[3] is a recently isolated member of the viscosin group of CLPs[1, 2]. It consists of a nonapeptide chain where the depsi bond involves the D-*allo*-Thr3 side chain, while the N-terminus is connected to a 3-hydroxydecanoic acid (HDA) moiety (Figure 1). It was found to display bacteriostatic activity mainly against Gram positive bacteria. Its crystal structure, revealed by X-ray diffraction of crystals obtained from acetonitrile solution[3], features a short left handed α-helix ranging between D-Gln2 and D-Leu5 followed by a three

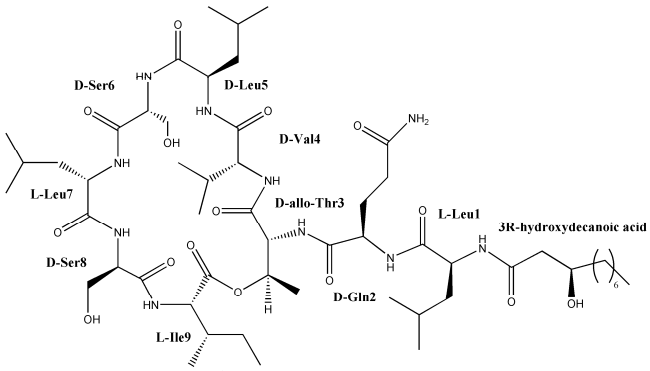

Figure 1. Chemical structure of pseudodesmin A.

[a] D. Sinnaeve, Dr. P. M. S. Hendrickx, Prof. Dr. J. C. Martins
NMR and Structure Analysis Unit
Department of Organic Chemistry
Ghent University
Krijgslaan 281 S4, B-9000 Gent (Belgium)
Fax: +32 (0)9 264 4972
E-mail: Davy.Sinnaeve@UGent.be, Jose.Martins@UGent.be

[b] Dr. J. Van hemel, Dr. E. Peys
Kemin Pharma
Atealaan 4H, B-2200 Herentals (Belgium)

[c] Prof. Dr. B. Kieffer
IGBMC
Biomolecular NMR group
1 rue Laurent Fries BP 10142, 67404 Illkirch CEDEX (France)

Supporting information for this article is available on the WWW under http://www.chemeurj.org/ or from the author.

residue loop connecting the C-terminus of the helix with the D-*allo*-Thr3 side chain to make the lactone bond

Members of the various CLP groups display a variety of moderate biological effects, including antimicrobial activity[2]. In several cases, the mechanism for this activity has been ascribed to the formation of passive transport ion pores in the cellular membrane[4, 5] in a fashion similar to what is generally described for (non cyclic) antimicrobial peptides (AMPs)[6, 7]. For instance, syringomycin, a CLP very different from the viscosin group members, is described to form pores that allow Ca^{2+} to transport passively, initiating phosphorylation of several proteins and disturbing ATPase function[5]. Within the viscosin group, the White Line Inducing Principle (WLIP)[8] is a close analogue of pseudodesmin A, differing only in a D-Gln to D-Glu substitution. It has been shown to insert itself within model membranes[4], while its pore forming capability was demonstrated on erythrocytes using osmotic protectants[9]. The crystal structures of WLIP and pseudodesmin A are highly similar and both are amphipatic in nature, with a large amount of the molecular surface covered by hydrophobic side chains and a smaller surface by hydrophilic ones[3]. Taking these elements together, the hypothesis of a membrane insertion followed by *in situ* assembly into a supramolecular ion pore structure would appear as a plausible explanation for their biological function.

A common procedure to study the structure and behaviour of a membrane-bound peptide by solution NMR methods is to use artificial lipid micelles or bicelles[10]. However, due to the limited amount of material available and the desirability to recuperate the product, an alternative approach was chosen for pseudodesmin A. In this work, pseudodesmin A was dissolved in simple apolar organic solvents, such as chloroform, thereby inducing strong self-association behaviour. The concentration and solvent polarity dependency of the self-association is initially studied using translational diffusion NMR measurements. To further examine the main aspects of the supramolecular structure in chloroform, the solution structure of pseudodesmin A was first determined by NMR in acetonitrile, where no self-association occurs. The solution structure is found to be very similar to the crystal structure and is further shown to be mostly preserved in chloroform. Starting from this solution structure, intermolecular rOe correlations are used to identify intermolecular contact surfaces, from which a possible assembly scenario relevant to pore formation is derived. In addition, a long standing issue regarding the marked difference between the crystal and solution conformation of WLIP is resolved by showing that it is linked to the occurrence of conformational exchange due to the choice of DMSO as solvent.

Results

Pseudodesmin A self-associates in apolar solvents: When pseudodesmin A is dissolved at 2 to 3 mM concentration in a variety of solvents, a single, well-defined set of resonances is observed in all cases. However, the line-width properties of the pseudodesmin A resonances are highly dependent on the solvent used. Figure 2 compares the aliphatic region of the 1D ^1H spectra recorded in acetonitrile and chloroform solution, from which it is clear that all resonance line widths are significantly increased in chloroform. Similar effects were also apparent in other apolar solvents that were tested, dioxane and benzene, while in the more polar DMF or acetone this was not the case (supporting information). Line-

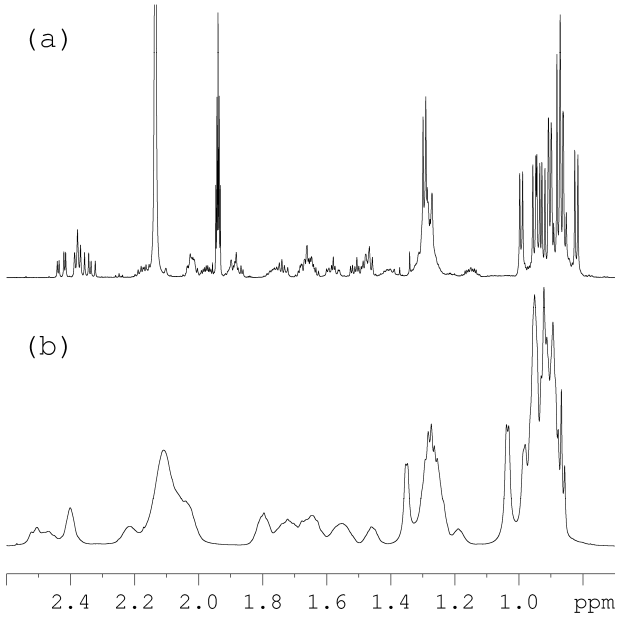

Figure2. Aliphatic region of the 700.13 MHz ^1H NMR spectrum in (a) ca 2mM acetonitrile and (b) 20.5 mM chloroform.

broadening generally reflects an increase in the transverse relaxation rate R_2. Since all pseudodesmin A resonances are affected equally and the effect does not seem to increase with the magnetic field, an exchange process is not the dominant source for the line broadening. Therefore it appears most likely that an increase in the global molecular rotational correlation time τ_c lies at the basis of this phenomenon, since $R_2 \sim \tau_c$ and the latter is dependent on both solvent viscosity and molecular size. Though the viscosity of chloroform is about 1.5 times higher than acetonitrile, it is insufficient to explain the strong line width changes observed. This is confirmed by measuring the translational diffusion coefficient of pseudodesmin A using PFG-NMR techniques and calculating the hydrodynamic (or Stokes) radius R_H using the Stokes-Einstein relation and the known viscosity of each solvent[11] (Table 1). In acetonitrile solution, the value of 7.2 Å is in agreement with the dimensions of a pseudodesmin A molecule as determined from its crystal structure. However, in chloroform the observed R_H value is both much higher and concentration dependent. This confirms that pseudodesmin A self-associates into larger aggregates when exposed to apolar solvents, while in acetonitrile or other polar solvents the compound remains in a monomeric state. At the highest concentration in chloroform measured (20.5 mM), the R_H value is at 38.2 Å, which constitutes a more than five fold increase compared to acetonitrile. When lowering the concentration down to 3.0 mM, the hydrodynamic radius is reduced to 18.4 Å, which is still much higher than in acetonitrile. It is only at the much lower concentration of 0.06 mM that a value close to the one in acetonitrile is found. This concentration dependent change is also reflected by the clear sharpening of all the resonances. It should be noted that only a single set of resonances is visible throughout the entire concentration range investigated. Also, all diffusion induced resonance intensity decays in the PFG-NMR experiments are monoexponential. Together with the concentration dependence of R_H, the data in chloroform is consistent with a process where an indefinite self-association occurs in which individual pseudodesmin A molecules are in a fast exchange equilibrium with a collection of supramolecular complexes of varying size. This concentration dependent size-distribution expected for such association process is then reflected via an averaged diffusion coefficient.

Table 1. Translational diffusion coefficients and hydrodynamic radii of pseudodesmin A

Solvent	D [$\mu m^2 s^{-1}$][a]			R_H [Å][b]
acetonitrile	816.8	±	4.4	7.2
chloroform				
20.5 mM	106.6	±	0.3	38.2
3.0 mM	220.6	±	1.4	18.4
0.06 mM	468.0	±	13.5	8.7

[a] 95% confidence intervals obtained using a Monte Carlo procedure. [b] For the hydrodynamic radius calculation, the viscosity is assumed to be 0.369 mPa·s for acetonitrile and 0.537 mPa·s for chloroform[11].

To further assess the effect of solvent polarity, a solvent titration experiment at constant pseudodesmin A concentration was performed starting from a solution of ca 2 mM pseudodesmin A in chloroform to which a pseudodesmin A solution in acetonitrile of exactly the same concentration was gradually added to keep the concentration constant. The evolution of the apparent diffusion coefficient of pseudodesmin A is plotted in Figure 3. The diffusion coefficient steadily increases with the acetonitrile volume percent, until at 13% a value is reached of 484.7 ± 2.8 $\mu m^2 s^{-1}$, which is similar to the diffusion coefficient of 468.0 ± 13.5 $\mu m^2 s^{-1}$ for the 0.06 mM chloroform solution. The diffusion coefficient of added TMS in the sample was followed as well, showing almost no variation (supporting information), and thereby confirming that no significant change in viscosity occurs between the different solvent mixtures. The gradual decrease of the self-association with increasing acetonitrile volume percent clearly demonstrates that the self-association equilibria and thus the size and distribution of the supramolecular structures in solution can be controlled by changing the overall polarity of the solvent.

Solution structure of pseudodesmin A: To gain insight into the organization of the supramolecular structure and more particularly into the contacts that exist between the molecular units, the conformation of the individual monomers within the structure must first be known. Although the crystal structure of pseudodesmin A was previously determined[3], it was important to assess the conformation in solution. This is because WLIP, a close analogue of pseudodesmin A and the only viscosin group member for which a solution structure is available, has been reported to adopt a conformation in solution that is markedly different from the crystal structure[8, 12]. Determining the monomer structure directly in chloroform is complicated however since intra- and intermolecular contributions to the nOe correlations cannot *a priori* be distinguished. Given that the level of dilution required to ensure a monomeric state for pseudodesmin A in chloroform is too large for comfortable NMR based conformational analysis, we first considered determining the structure in acetonitrile solution where the molecule exists in monomer form even at higher concentrations.

Towards this end, 127 rOe distance restraints were collected and used as input in a restrained molecular dynamics simulation followed by energy optimization, the result of which is represented by an ensemble of the 40 lowest energy conformers in Figure 4. The energies and residual violation statistics of the refined conformers (supporting information) indicate a low energy ensemble in good agreement with the experimental data. Only the HDA alkyl chain

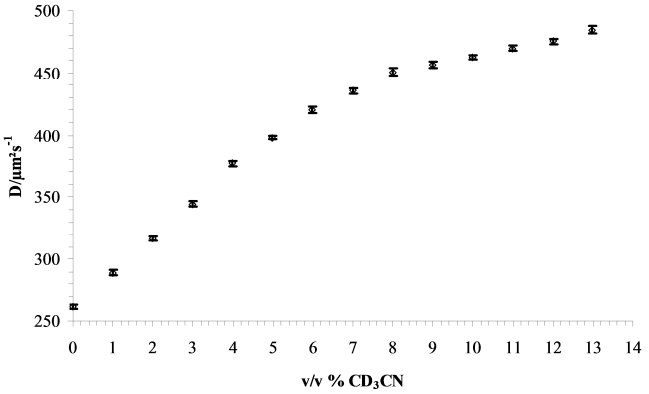

Figure 3. Titration of a pseudodesmin A sample in chloroform with acetonitrile. Error bars represent 95% confidence intervals obtained using a Monte Carlo procedure. The tabulated data points can be found in the supporting information.

and the Leu1 residue present significant conformational variability over the ensemble. This is further illustrated by the low torsion angle order parameter[13] of the L-Leu1 φ angle (0.40), while all other φ and ψ torsion angles possess order parameters of at least 0.99. Finally, the RMSD value of 0.91 ± 0.21 Å over all 63 heavy atoms except the HDA moiety further drops to 0.12 ± 0.08 Å when only the 7 endocyclic residues are considered. This very low RMSD value should however not necessarily be interpreted as a measure of the actual structural definition in solution, but rather indicates the limited variability allowed by the many constraints imposed during the structure calculation. Importantly however, the overall solution conformation of pseudodesmin A is highly similar to the crystal structure[3], with an RMSD value of 0.14 Å obtained upon superposition of the 15 backbone atoms of the Leu1-Ser6 segment. Small differences are more apparent from the individual φ/ψ backbone angles collected in Table 2. These show that D-Ser6 is more in line with the α-helix rather than being involved in a type I' β-turn as is the case in the crystal structure. The hydrogen bonds that define the α_L helix are clearly present both in the crystal and solution structures. The loop adopts a somewhat different orientation (Figure 5), reflected in the altered φ/ψ values of D-Ser8 and L-Ile9. This is accompanied with some changes in the hydrogen bond network (Table 3) involving the loop residues. Careful analysis indicates that these differences should be attributed to the presence of intermolecular hydrogen bonds in the crystal structure, such as the Ile9 NH→Leu5 CO hydrogen bond. All of this notwithstanding, the overall structure obtained by both methods is quasi identical

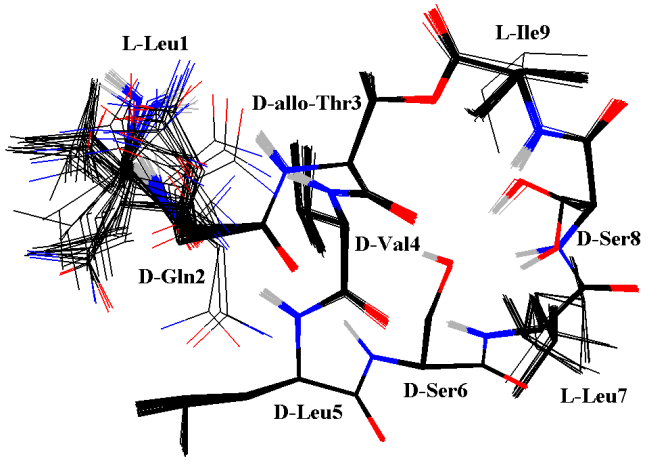

Figure 4. Overlay of the 40 lowest energy structures of pseudodesmin A. The HDA moiety has been removed for clarity.

Table 2. φ and ψ torsion angles of pseudodesmin A solution structure compared with the crystal structure

		Leu1	Gln2	Thr3	Val4	Leu5	Ser6	Leu7	Ser8	Ile9
NMR	φ [a]	--[b]	61.4	69.47	64.01	55.5	65.15	-66.01	107	-118.1
	ψ [a]	62.07	38.36	37.9	46.52	45.26	22.38	-24.84	18.65	-4.09
Crystal	φ	-60.9	57.09	63.33	61.78	63.12	98.05	-66.43	150.66	-65.99
	ψ	122.69	28.52	40.47	48.59	31.68	1.01	-50.62	-41.21	-6.31

[a] Averaged value of the 40 lowest energy structures. The average of an angle α is defined using the average of the cosine and sine values over all structures: [α]=arctan[<sin(α)>/<cos(α)>]+k180°, with k=0 if <cos(α)> > 0; k=1 if <cos(α)> < 0 and <sin(α)> > 0; k=-1 if <cos(α)> < 0 and <sin(α)> < 0. [b] Value omitted due to low order parameter (0.40).

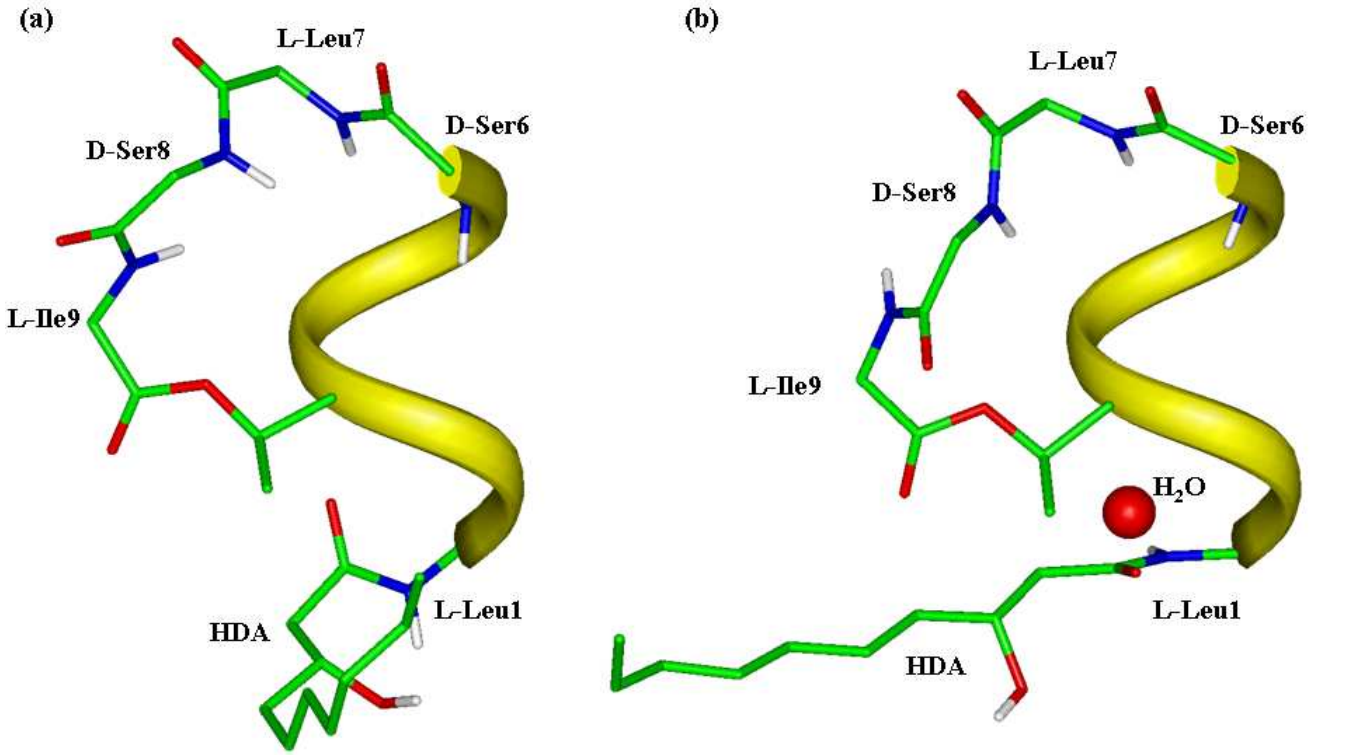

Figure 5. Comparison of the solution (a) and crystal (b) structures of pseudodesmin A showing only the backbone atoms. The helix is shown as a ribbon (N→C from bottom to top), while the Leu7-Ile9 loop can be seen making the connection between the C-terminus of the helix and the Thr3 side chain. Note that in the loop Ile9 is oriented differently between both structures.

(Figure 5), in marked contrast with the WLIP case (*vide infra*).

The results of a $^{1}H/^{2}H$ exchange experiment in a CD_3CN/D_2O mixture are in good agreement with the solution structure. As can be seen from Table 4, slow exchange rates on the order of hours to days are found for the amide hydrogens in the Leu5–Ile9 segment. While the Ile9 amide is not involved in any hydrogen bond in the solution structure, its NH bond points inward from the loop to the helix, making it totally solvent inaccessible. The higher exchange rates of both Ser amide hydrogens are most probably caused by participation of the side chain hydroxyl groups in the exchange process with the solvent. The relatively fast exchange rates found for the Leu1, Gln2 and Thr3 amide hydrogens agree with their location at the N-terminal side of the α_L-helix. Although the solution structure predicts a hydrogen bond involving Val4 NH and HDA CO, the Val4 amide hydrogens exchanges fairly rapidly. This suggests that the conformation of the exocyclic part is more dynamic. Altogether, the data indicate that the solution structure in acetonitrile is well-defined and considerably rigid.

An important question is the extent to which the solution structure of pseudodesmin A in acetronitrile, is maintained within the supramolecular structures formed through self-assembly in chloroform. A conformation sensitive parameter that unlike the nOe does not suffer from intra- or intermolecular ambiguity is the $^{3}J_{HH}$ scalar coupling constant, with the most relevant being the $^{3}J_{HNH\alpha}$ couplings reflecting the backbone φ torsion angles. As seen in Table 5, neither their values nor the torsion angles derived from them change to an extent that would indicate major local or global changes in the backbone conformation between the two solvents. Therefore, the solution structure of pseudodesmin A in acetonitrile is a valid model to explore the supramolecular assembly.

Table 3.Overview of pseudodesmin A solution structure hydrogen bonds

Donor	Acceptor	d_{D-A} [Å][a]	angle [°][a]
Val4 NH	HDA CO	2.88	158.95
Leu5 NH	Leu1 CO	2.97	172.42
Ser6 NH	Gln2 CO	2.85	158.70
Ser6 OH	Thr3 CO	2.71	148.36
Leu7 NH	Val4 CO	3.16	154.76
Ser8 NH	Ser6 OH	2.92	158.71
Ser8 OH	Ser6 OH	2.66	165.77

[a] Hydrogen bonds are considered to have a donor-acceptor bond length of at most 3.4 Å and a bond angle of at least 140°.

Table 4. $^{1}H/^{2}H$ Exchange kinetics

Amide resonance	k [s^{-1}][a]	$t_{1/2}$[b]		
Leu1	2312.15			5m
Gln2	2327.39			5m
Thr3	1366.82			9m
Val4	923.33			14m
Leu5	3.03	2d	18h	8m
Ser6	75.83		2h	39m
Leu7	1.63	5d	2h	57m
Ser8	27.95		7h	6m
Ile9	1.21	6d	22h	12m
Gln2 NH_2 1	836.84			14m
Gln2 NH_2 2	805.75			15m

[a] Exchange rate constants k are obtained by fitting the signal intensity decay in function of time t to the equation $I(t) = I(0)[(1 - \alpha)\exp(-kt) + \alpha]$, with α the remaining protonated fraction when equilibrium is achieved. [b] The exchange half-lives $t_{1/2}$ (expressed in days (d), hours (h) and minutes (m)) are calculated as $t_{1/2} = -\ln[(0.5 - \alpha)/(1- \alpha)]/k$.

Indications of intermolecular contacts in the supramolecular structure: A comparison of the NMR data between the two solvents can provide information on how the supramolecular structure is organized. Since the conformation of the individual monomer units within the supramolecular structure is similar to the acetonitrile solution structure, all spatial ^{1}H-^{1}H proximity correlations observed in chloroform that cannot be explained by this conformation can be interpreted as intermolecular contacts. 2D NOESY spectra are useless for this purpose, since the large molecular size leads to excessive spin-diffusion even at short mixing times. This is in sharp contrast with NOESY spectra measured in acetonitrile, further emphasizing the strong difference in global rotational correlation time between both solvents (supporting information). Because of this, the possibility to distinguish direct intermolecular contacts from intramolecular nOe contacts is lost. The use of 2D ROESY is therefore preferred here. While inherently less sensitive due to the contribution from efficient T_2 relaxation during the 40 ms spin-lock time used here, it has the advantage of a greatly reduced degree of spin diffusion, whereas its presence can be recognized by the occurrence of a sign inversion of the rOe cross-peak[16].

Table 5.comparison of scalar couplings between chloroform and acetonitirile

^{3}J	J_{CD3CN} [Hz]	J_{CDCl3} [Hz]	difference [Hz]	torsion angle difference[a] [°]
Leu1 $H^{N}H^{\alpha}$	5.7	6.0	-0.4	--[b]
Gln2 $H^{N}H^{\alpha}$	4.0	3.1	0.9	-7.6
Thr3 $H^{N}H^{\alpha}$	7.5	6.2	1.3	-9.7
Val4 $H^{N}H^{\alpha}$	6.3	4.9	1.4	-10.7
Leu5 $H^{N}H^{\alpha}$	4.3	2.9	1.3	-11.4
Ser6 $H^{N}H^{\alpha}$	8.5	8.0	0.5	-4.4
Leu7 $H^{N}H^{\alpha}$	6.5	4.4	2.2	16.3
Ser8 $H^{N}H^{\alpha}$	9.1	8.8	0.3	-3.1
Ile9 $H^{N}H^{\alpha}$	10.7	9.8	0.9	--[c]
Thr3 $H^{\alpha}H^{\beta}$	10.7	10.9	-0.2	-1.3

[a] Torsion angles were calculated using a Karplus curve relation with parameterization according to Vuister *et al* for $H^{N}H^{\alpha}$ couplings[14] and Demarco *et al* for the $H^{\alpha}H^{\beta}$ coupling[15]. [b] Not compared since the bond is assumed to be flexible in acetonitrile solution. [c] Ile9 $H^{N}H^{\alpha}$ coupling constant in chloroform is out of reach of the Karplus curve, most likely because the unusually attached ester group influences the correct parameterization of the curve.

After cataloguing all rOe correlations in chloroform and confronting them with the solution structure, several contacts were revealed that cannot be expected to arise from a short distance through space or in residue sequence within a single monomer (Table 6). Note that mainly backbone protons are involved, with the H^{N} protons of the exocyclic Leu1 and Gln2 contacting the H^{α} protons of the loop located at the opposite end of the monomer structure. These particular amides are not involved in any intramolecular hydrogen bonding in the solution structure, which is also true for the carbonyl groups in the loop. Therefore these rOe contacts suggest that the interaction between monomers may be mediated by intermolecular hydrogen bonds involving those two regions. Also noteworthy in this context are the contacts between the side chain amide protons of Gln2 with the loop backbone and the Ser side chains, which may indicate an intermolecular interaction between those hydrophilic side chains.

Another probe sensitive to intermolecular contacts is the chemical shift. A solvent titration was performed starting from a solution in chloroform and stepwise adding acetonitrile. The ^{1}H, ^{13}C and ^{15}N chemical shifts were followed from ^{1}H-^{13}C gHSQC and ^{1}H-^{15}N gHSQC spectra recorded for each solvent mixture. The changes in chemical shift are shown in Figure 6 (for tabulated values, see supporting information). The most notable changes (>0.3 ppm) in the $^{1}H/^{13}C$ chemical shifts occur mainly at those positions where intermolecular rOe contacts were detected as well (Leu7 CH^{α}, Ser8 CH^{α} and CH_2^{β}, HDA CH_2^{α}). Overall, no strong

Table 6. Intermolecular rOe contacts between ^{1}H resonances in chloroform

resonance 1		resonance 2		d_{intra} [Å][a]	rOe[b]
HDA	H^{α}	Ser8	H^{α}	9.8	strong
HDA	H^{α}	Ser6/Ile9[c]	H^{α}	9.8/6.6	weak
HDA	H^{γ}	Ser8	H^{α}	10.3	strong
Leu1	H^{N}	Ser6	H^{β}	9.0	weak
Leu1	H^{N}	Leu7	H^{α}	12.5	strong
Leu1	H^{N}	Ser8	H^{α}	12.7	strong
Leu1	H^{N}	Ser8	OH^{γ}	9.9	intermediate
Leu1	H^{N}	Ile9	H^{β}	9.3	strong
Leu1	H^{N}	Ser6/Ile9[c]	H^{α}	10.7/10.0	intermediate
Gln2	H^{N}	Leu7	H^{α}	11.1	strong
Gln2	H^{N}	Ser8	H^{α}	11.6	strong
Gln2	H^{N}	Ser8	OH^{γ}	8.3	intermediate
Gln2	H^{N}	Ser6/Ile9[c]	H^{α}	8.5/9.9	weak
Gln2	H^{N}	Ile9	H^{β}	9.8	strong
Gln2	NH_2 E[d]	Ser6	H^{β}	7.3	weak
Gln2	NH_2 Z[d]	Ser6	H^{β}	8.4	weak
Gln2	NH_2 E	Ser6	OH^{γ}	8.8	intermediate
Gln2	NH_2 Z	Ser6	OH^{γ}	9.5	weak
Gln2	NH_2 E	Leu7/Leu5[c]	H^{α}	13.5/10.5	intermediate
Gln2	NH_2 Z	Leu7/Leu5[c]	H^{α}	14.3/11.0	intermediate
Gln2	NH_2 E	Ser8	H^{α}	13.1	strong
Gln2	NH_2 Z	Ser8	H^{α}	13.9	strong
Gln2	NH_2 E	Ser8	OH^{γ}	9.4	weak
Gln2	NH_2 Z	Ser8	OH^{γ}	10.3	weak
Gln2	NH_2 E	Ile9	H^{β}	12.7	weak
Gln2	NH_2 Z	Ile9	H^{β}	12.6	weak

[a] Intramolecular distance between the hydrogen atoms within the solution structure. [b] rOe intensity in chloroform solution. [c] Ambiguous assignment. [d] Discrimination of E and Z protons based on Gln2 NH_2 – Gln2 CH_2^{γ} rOe intensities.

changes are detected at the level of the hydrophobic side chains, where the chemical shift perturbations of all methyl groups, except Thr3 CH_3^{γ}, lie between 0.02 ppm and 0.13 ppm. Important perturbations in $^{1}H/^{15}N$ chemical shifts for the Leu1 and Gln2 NH groups are also in agreement with the intermolecular rOe results, while the changes seen for the Leu7 and Ser8 NH groups are a likely consequence of the respective residues being involved in the same intermolecular contact surface. The origin for the considerable changes at the level of the Val4 and Leu5 NH is less obvious. It is conceivable that the association process induces changes in the intramolecular hydrogen bond strength, leading to the observed changes in the environment sensitive amide chemical shift. However, from their location in the structure we notice that they do not participate in the proposed interface.

Behaviour in DMSO solution: The ^{1}H and ^{13}C NMR spectra of pseudodesmin A at 298 K show clear indications of a conformational exchange process involving two or more conformers. First, several resonances show severe line broadening (supporting information), including most H^{N} resonances (most notably Gln2, Ser6 and Leu7), several H^{α} resonances (e.g. Ile9, Leu5) and even several ^{13}C carbonyl and C^{α} resonances. Since the line broadening is not equally present on all resonances as is the case in chloroform, it is most likely caused by a conformational exchange process that is near a coalescence situation where the exchange rate is on the same order of magnitude of the frequency difference between the different states for those spins ($k_{ex} \sim \Delta\nu$). This is confirmed by noting that the resonances sharpen as the temperature is increased (k_{ex} increases) or the magnetic field strength is lowered ($\Delta\nu$ decreases) (supporting information), thus moving the system to a fast exchange situation ($k_{ex} > \Delta\nu$). In addition, the temperature dependence of the H^{N} resonance of Leu1, Gln2 and Ser8 is non-linear, with an initial positive slope that is reversed into the regular negative one at higher temperatures (supporting information). Due to the high melting temperature of DMSO, it is impossible to reach the slow exchange regime even at 700 MHz. Therefore, the exact number and nature of conformational states cannot be established by solution NMR. Nevertheless, there are clear differences in the pattern of rOe contacts in DMSO measured at 323 K, compared to acetonitrile. Most notable are the absence of any correlations between the Leu7 and Val4 residues and the presence of correlations between the Ser6 H^{α} proton and Ile9 CH_2^{γ} and CH_3^{δ} protons. These observations cannot be explained from either the solution or crystal structure.

Discussion

Conformation of pseudodesmin A, WLIP and other viscosin group members: Previously, we established that the crystal structure of pseudodesmin A and WLIP, a viscosin group member that features a D-Glu2 residue instead of D-Gln2, are quasi identical[3]. Here, we show that the solution structure of pseudodesmin A is mostly similar to these crystal structures, at least in acetonitrile solution. This contrasts with the solution structure of WLIP, previously determined by Mortishire-Smith *et al* in DMSO[8] where significant differences were reported between the crystal and solution structure. For instance, the WLIP solution structure features a type II β-turn involving a hydrogen bond between the Ser6 NH and the Ile9 carbonyl. This apparent contradiction can be attributed to the difference in solvent used in both studies. When pseudodesmin A is dissolved in DMSO, several effects described for WLIP are observed as well, including non-linear temperature coefficients for the Leu1, Glu2 and Ser8 H^{N} resonances and the observation of nOe contacts between Ser6 and Ile9. Also, the same H^{N} resonances appear broadened due to conformational exchange at room temperature. Keeping in mind that pseudodesmin A can be considered the amide form of WLIP, we propose that both WLIP and pseudodesmin A experience similar conformational exchange in DMSO. Importantly, the validity of the solution conformation of WLIP in DMSO must therefore be questioned, and should not be considered to have biological relevance as it was determined from constraints that are weighted by several conformers. When imposed during structure calculations, these lead to virtual conformations, thereby explaining the discrepancy with the WLIP crystal structure.

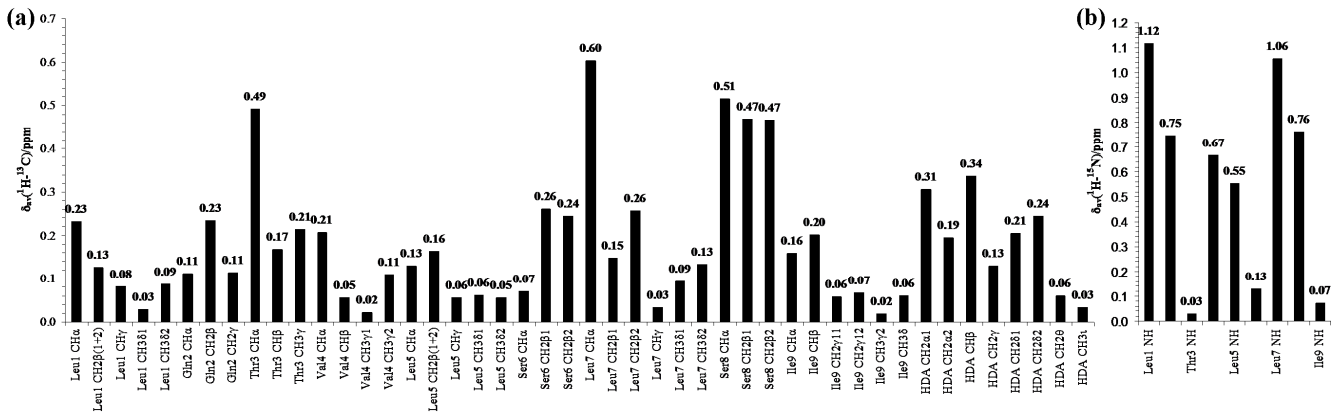

Figure 6. Average $^{1}H/^{13}C$ (a) and $^{1}H/^{15}N$ (b) chemical shift perturbations resulting from a titration of a chloroform solution with acetonitrile. For a tabulation of the values, see the supporting information.

When pseudodesmin A was dissolved in other solvents such as acetone or DMF, the ^{1}H chemical shifts remained mostly similar to acetonitrile and no line broadening was apparent. The reason for the unique behaviour in DMSO can most probably be related to its very strong hydrogen bonding acceptor capability, even more so than amide carbonyls[17]. In DMSO solution therefore, the solvent acts as a strong competitor for hydrogen bond interactions and effectively as a denaturant for the cyclic peptide. Because DMSO is a very polar molecule, it would be unreasonable to connect the behaviour of pseudodesmin A in this solvent to its self-association properties, since it would contradict the observed effect of the solvent polarity on the self-assembly.

Several viscosin group members (pseudodesmin B[3], WLIP and the pseudophomins[18]) vary only slightly in the nature of the side chains compared to pseudodesmin A. Therefore it can confidently be assumed that the conformation and behaviour in solution is similar for all these compounds. The other viscosin group members differ as they possess at the 5 position an L instead of D configuration. Since no solution or crystal structures are know for any of these compounds, the direct impact on the helix structure cannot yet be assessed.

Structural proposal for the supramolecular assembly: It has often been postulated that the biological function and antimicrobial mechanism of CLPs is related to the formation of passive transport ion pores in the cellular membranes[5]. Although a simple organic solvent environment should not be considered a good mimic for the interior of biological membranes, both share an apolar character. Given the nature and stability of the pseudodesmin A monomer structure, it is reasonable to expect that inside the membrane bilayer, the conformation would also be preserved and thus the same supramolecular structures observed as in apolar solvents will be formed with dimensions naturally imposed by the confines of the membrane bilayer. To the best of our knowledge, this represents the first attempt to link or confront the pore forming capacity of CLPs, such as WLIP, to their individual crystal or solution structures. Based on the pseudodesmin A solution structure in acetonitrile, the observation that its main structural elements are retained in chloroform and using the data concerning intermolecular contacts and chemical shift perturbation, a first model for the supramolecular self-association and therefore the pore forming capacity can be elaborated (Figure 7).

We suggest that two types of distinct intermonomer interactions occur in the assembly of the pore. First, the solution structure of pseudodesmin A shows a clear amphipatic character, with all hydrophobic and hydrophilic residues occurring at positions in the sequence that arrange their side chains on opposite sides of the molecule. This creates a large hydrophobic surface, comprised of all Leu, Ile and Val side chains. A smaller hydrophilic surface includes both the Ser and the Gln residue side chains. When inserted into an apolar solvent or membrane environment, pseudodesmin A molecules can be expected to pack their hydrophilic surfaces together while extending the hydrophobic surfaces outward so to minimize energetically unfavourable hydrophobic-hydrophilic contacts. This idea has been described previously for many AMPs in general[6], and finds additional support in the previously made observation that the hydrophobic and hydrophilic residue positions are strongly conserved within the viscosin group[3]. However, such an aggregation would be insufficient to explain the huge change in size observed in apolar environments. In addition, the dimensions of pseudodesmin A, which are on the order of 10-15 Å are too small to span the membrane bilayer (±45 Å). Therefore an additional degree of supramolecular association is proposed.

Inherently, the helix structure possesses free CO and NH groups at its C- and N-terminal ends respectively, while in addition pseudodesmin A has more free CO groups in its loop structure. This creates a build-up of opposite charge at opposing sides of the molecule, effectively creating a macrodipole[19]. In an apolar solvent or membrane, this can lead to an electrostatically driven alignment of molecules along a direction closely parallel with the helix, most likely with intermolecular NH-CO hydrogen bonds. This is supported by the observed strong intermolecular rOe contacts of the Leu1 and Gln2 H^{N} with the Leu7 and Ser8 H^{α}. In this manner the 'length' necessary for the pore to span the cellular membrane is created. In addition, it would explain why the self-association is not observed in polar environment, since the polar solvent molecules would quench the need for such alignment.

The formation of intermolecular amide hydrogen bonds gains further support by the results of a FT-infrared spectroscopy study combined with $^{1}H/^{2}H$ exchange of WLIP performed by Coraiola *et al*[4]. They detected the presence of non-hydrogen bonded amides in buffer solution, which seemed to decrease when dissolved in model membrane environment. As an alternative for a change in conformation of WLIP proposed by these authors, this could also be

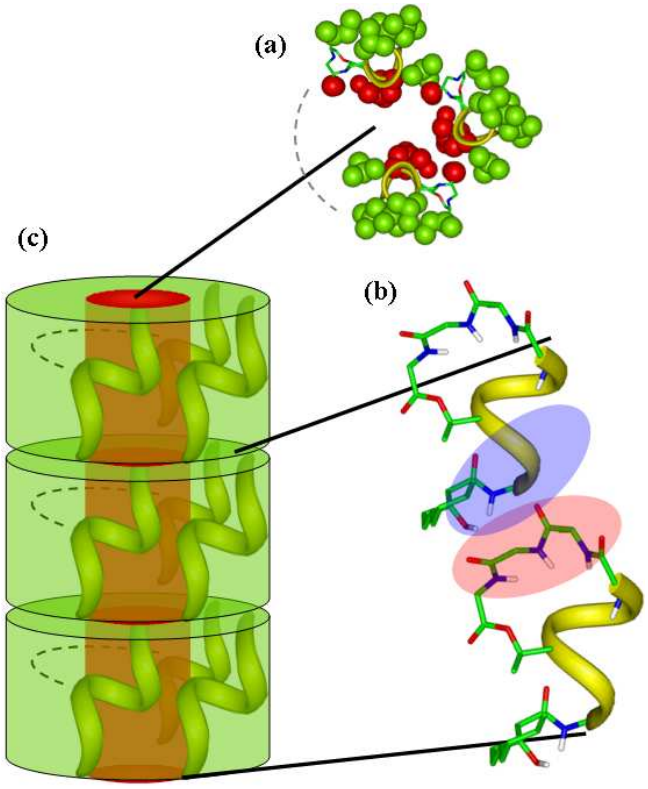

Figure 7. Illustration of the proposed model for the self-association. No actual residue specific intermolecular interactions or detailed arrangement of individual molecules are intended. (a) Top view of an undefined number of pseudodesmin A molecules aggregating their hydrophilic residue side chains (red) towards each other and directing the hydrophobic residue side chains (green) outward. (b) The free NH groups at the N-terminal end of the helix interact through electrostatic interaction with the free CO groups at the C-terminal end or the loop. (c) Both processes combined, a large supramolecular structure is formed with a hydrophilic interior and a hydrophobic exterior.

explained by intermolecular hydrogen bonding between the free NH groups of the N-terminal side of the helix of one molecular unit with the free CO groups of another unit.

With these two processes combined (Figure 7), a large structure forms that can span the membrane, with a hydrophilic interior allowing positively charged ions to coordinate with alcohol or free carbonyl groups, thus creating a channel through the membrane. The function of the HDA chain would then most likely be to increase membrane solubility or facilitate anchoring of the CLP in the membrane by tightly interacting with the lipid chains. The proposed model can be extended to other helix bearing CLPs with amphipatic structure, such as WLIP, the pseudophomins[20], amphisin[21] and tensin[22], which all possess a similar sequence to pseudodesmin A.

Experimental Section

NMR spectroscopy: All NMR measurements were performed on either a Bruker DRX spectrometer operating at a respective ^{1}H and ^{13}C frequency of 500.13 MHz and 125.76 MHz, or a Bruker Avance II spectrometer operating at a respective ^{1}H, ^{13}C and ^{15}N frequency of 700.13 MHz, 176.05 MHz and 70.94 MHz. In both cases, a $^{1}H,^{13}C,^{15}N$ TXI-Z probe was used, with z-gradients calibrated to respectively 56.1 Gcm^{-1} and 57.9 Gcm^{-1}. The sample temperature was set to 298.0 K unless otherwise mentioned. High quality NE-HP5-7 (New Era Ent. Inc) NMR tubes were used. [D_3]Acetonitrile (99.96%), [D_6]acetone (99.96%), [D_6]benzene (99.96%), [D]chloroform (99.96%) and tetramethylsilane (TMS) were purchased from Eurisotop, [D_7]DMF (99.5%) and [D_8]dioxane (99%) from Sigma Aldrich and [D_6]DMSO (99.96%) from Cambridge Isotope Laboratories. Pseudodesmin A was obtained as described previously [3].

Because the increased line-width of pseudodesmin A in chloroform prevented the direct extraction of scalar couplings from the 1D ^{1}H spectra, alternative techniques were required. The Thr3 $^{3}J_{H\alpha H\beta}$ scalar coupling in chloroform was obtained using a SERF experiment[23] at 500.13 MHz and 283.0 K, measured with 32 data points in the indirect dimension and processed with a squared cosine bell window function. All $^{3}J_{HNH\alpha}$ couplings in chloroform were obtained from a 3D HNHA experiment[14] at 700.13 MHz. This was measured with 2048 time domain points sampled in the direct dimension (F3), 32 time domain points in the indirect ^{1}H dimension (F2) and 16 time domain points in the indirect ^{15}N dimension (F1), while the spectral widths were set to 7.0 ppm for the ^{1}H dimensions and 6.6 ppm for the ^{15}N dimension. The low spectral width set for ^{15}N folded the spectrum in this dimension, allowing the peaks to be sufficiently resolved with the limited number of indirect time domain points measured. Resolution in F2 and F1 was improved via one order of forward linear prediction. Zero filling was performed until a 2048×256×256 matrix was obtained, which was Fourier transformed using squared cosine bell window functions and afterwards baseline corrected with 5th degree polynomials in each dimension.

All pseudodesmin A samples in chloroform, except for the titration experiments, had a layer of water on top to reduce evaporation over time (Experimental Liquid Sealing, ELISE)[24]. The concentrations in the chloroform samples listed in Table 1 were determined with ERETIC (Electronic Reference to assess in vivo Concentration)[25] using samples of menthol in chloroform as a reference.

Translational diffusion measurements experiments were performed with NMR using convection compensated sequences; either the standard Bruker double stimulated echo with bipolar gradients and Longitudinal Eddy current Delay (LED)[26] or a double stimulated echo with monopolar gradients with an extended phase cycle[27]. The diffusion encoding/decoding gradients were half sine bell shaped and were varied linearly between 2% and 95% of their maximum output over 32 increments. The duration of these gradients and the diffusion delay time were chosen so that at the highest gradient strength increment the intensity of the signals of interest was decreased to less than 10% of the lowest gradient strength increment. Diffusion coefficients were obtained by integrating the resonances of interest and fitting the data to the Stejskal-Tanner equation appropriate for these pulse sequences[26] and corrected for the non-rectangular gradient shapes. 95% error bars were obtained using a Monte Carlo procedure with 500 simulations[28].

^{1}H, ^{13}C and ^{15}N chemical shift perturbations were obtained during a second solvent titration experiment performed at 283.0 K and at 700.13 MHz from sensitivity improved ^{1}H-^{13}C and ^{1}H-^{15}N gHSQC spectra. Standard pulse sequences from the Bruker library were used. The ^{1}H-^{13}C gHSQC spectra were recorded with a spectral width of 10 ppm and 2048 time domain points in the direct ^{1}H dimension, while for the indirect ^{13}C dimension a spectral width of 90 ppm and 512 time domain points were used. The ^{1}H-^{15}N gHSQC spectra were set up using a spectral width of 5 ppm and 1024 time domain points for the ^{1}H dimension and a spectral width of 32 ppm and 256 or 128 time domain points for the ^{15}N dimension. The resolution of both spectra was improved through forward linear prediction. A zero-filling was performed until a 2048×2048 or 1024×1024 real data matrix was obtained for respectively the ^{1}H-^{13}C and ^{1}H-^{15}N gHSQCs. Before Fourier transformation, all spectra were multiplied with a squared cosine bell window function in both dimensions. Despite the lower sample temperature, solvent evaporation over time was inevitable due to the long measurement time required at natural abundance. Therefore the translational diffusion coefficient was used as a quantitative descriptor of the degree of self-association. To obtain a relevant chemical shift difference, the absolute value of the slope obtained through linear regression between chemical shift and diffusion coefficient (ranging between 178.5 $\mu m^2 s^{-1}$ and 436.3 $\mu m^2 s^{-1}$) was multiplied with the difference in diffusion coefficient over the entire titration experiment. The $^{1}H/^{15}N$ average chemical shift was calculated[29] as $\delta_{av} = \delta(^{1}H) + \delta(^{15}N)/5$, while the $^{1}H/^{13}C$ average was calculated as $\delta_{av} = \delta(^{1}H) + \delta(^{13}C)/2$ (supporting information).

For the detection of intermolecular rOe contacts, a 40 ms mixing time 2D ^{1}H-^{1}H off-resonance ROESY spectrum[30] in a ca 20 mM pseudodesmin A solution in chloroform was performed at 283.0 K at 700.13 MHz.

Acetonitrile solution structure determination: Off-resonance ROESY[30] spectra were recorded at 500.13 MHz with mixing times varying between 75 ms and 400 ms to establish the linearity of the rOe build-up. A value of 200 ms was found to be the optimal mixing time for collecting distance restraints in acetonitrile. A 200 ms off-resonance ROESY experiment at 700.13 MHz performed in a 2 mM solution in [D_3]acetonitrile was subsequently recorded. All relevant cross peaks were integrated using the CCPNMR (v1.0 release 12) software[31] and corrected for multiplicity[16]. The conversion of rOe intensities into distances was calibrated against the average of the integrals of the rOe intensities between the β methylene protons of Leu5, Leu7, Ser8 and Ile9 and assuming a fixed distance of 1.74 Å[16]. All distances were increased by 10% prior to the addition of pseudo atom corrections for groups of equivalent or non-stereo assigned protons[16]. In total, 127 distance restraints were obtained in this way. These were enforced using a flat-bottomed harmonic potential with a force constant of 10 $kcal \cdot mol^{-1} Å^{-2}$ and a maximum energy penalty of 1000 $kcal \cdot mol^{-1}$. In addition, all

peptide bonds were restrained to their trans configuration by adding restraints to the ω torsion angle with a force constant of 100 kcal·mol^{-1}rad^{-2} whenever the deviation from the ideal 180º exceeded 5º. These restraints (supporting information) were used as input for restrained molecular modelling using the cff91 force field[32] within DISCOVER 2.98 (Accelrys, San Diego, CA, USA) running on an IBM Intellistation ZPro under Redhat Linux WS4. First, a set of 100 starting structures was obtained by sampling every 5 ps of the last 500 ps of a 550 ps unrestrained molecular dynamics (MD) simulation at 1000 K. Each was subjected to 100 steps of steepest descents energy minimization (EM) prior to restrained molecular dynamics (rMD) simulation using a simulated annealing protocol. Starting at 1000 K, the interproton distance restraints were gradually enforced on each structure in the initial set while cooling down the system in 150 K steps to 300 K with 1 ps rMD simulations at each temperature. The progression of the weighting constants for the experimental restraints was 0.1, 0.3, 0.7, 0.9 and 1.0. At 300 K an additional 3 ps rMD was performed. The energy of the conformation thus obtained was subsequently optimized by 100 steps of steepest descents restrained energy minimization (rEM) followed by conjugate gradients rEM until the maximum gradient of the cff91 energy was smaller than 0.001 kcal·mol^{-1}Å^{-1}. A subset of 40 structures with minimal energy was selected to represent the conformation of pseudodesmin A. The structure was confronted against ^{1}H-^{2}H amide exchange rates for validation. These were obtained by adding 61.1 µl of D_2O to a ca 8 mM solution of pseudodesmin A in 550 µl [D_3]acetonitrile at 298 K and monitoring the signal intensities of all exchangeable proton resonances over a 6 day period.

Acknowledgements

The Fund for Scientific Research – Flanders (FWO-Vlaanderen) is gratefully acknowledged for a PhD fellowship to D.S. and various equipment grants (G.0365.03, G.0064.07) to J.C.M. P.M.S.H. acknowledges the IWT Flanders for a PhD SBO-grant. The 700 MHz equipment of the Interuniversitary NMR Facility was financed by Ghent University, the Free University of Brussels (VUB) and the University of Antwerp via the 'Zware Apparatuur' Incentive of the Flemish Government. This research is supported by the NMR Scientific Research Community of the FWO.

[1] O. Nybroe and J. Sorensen in *Production of cyclic lipopeptides by fluorescent pseudomonads*, *Vol. 3* (Ed. J.-L. Ramos), Kluwer Academic/Plenum Publishers, New York, **2004**, pp. 147-172.

[2] J. M. Raaijmakers, I. de Bruijn and M. J. D. de Kock, *Mol. Plant-Microbe Interact.* **2006**, *19*, 699-710.

[3] D. Sinnaeve, C. Michaux, J. Van hemel, J. Vandenkerckhove, E. Peys, F. A. M. Borremans, B. Sas, J. Wouters and J. C. Martins, *Tetrahedron* **2009**, *65*, 4173–4181.

[4] M. Coraiola, P. Lo Cantore, S. Lazzaroni, A. Evidente, N. S. Lacobellis and M. Dalla Serra, *Biochim. Biophys. Acta, Biomembr.* **2006**, *1758*, 1713-1722.

[5] M. L. Hutchison, M. A. Tester and D. C. Gross, *Mol. Plant-Microbe Interact.* **1995**, *8*, 610-620.

[6] S. R. Dennison, J. Wallace, F. Harris and D. A. Phoenix, *Protein Pept. Lett.* **2005**, *12*, 31-39.

[7] K. V. R. Reddy, R. D. Yedery and C. Aranha, *Int. J. Antimicrob. Agents* **2004**, *24*, 536-547.

[8] R. J. Mortishire-Smith, J. C. Nutkins, L. C. Packman, C. L. Brodey, P. B. Rainey, K. Johnstone and D. H. Williams, *Tetrahedron* **1991**, *47*, 3645-3654.

[9] P. Lo Cantore, S. Lazzaroni, M. Coraiola, M. Dalla Serra, C. Cafarchia, A. Evidente and N. S. Iacobellis, *Mol. Plant-Microbe Interact.* **2006**, *19*, 1113-1120.

[10] G. S. Wang, *Curr. Org. Chem.* **2006**, *10*, 569-581.

[11] *Handbook of Chemistry and Physics 90th Edition* (Ed. D. R. Lide), CRC Press, Boca Raton, FL., **2009-2010**.

[12] F. S. Han, R. J. Mortishire-Smith, P. B. Rainey and D. H. Williams, *Acta Crystallogr., Sect. C: Cryst. Struct. Commun.* **1992**, *48*, 1965-1968.

[13] S. G. Hyberts, M. S. Goldberg, T. F. Havel and G. Wagner, *Protein Sci.* **1992**, *1*, 736-751.

[14] G. W. Vuister and A. Bax, *J. Am. Chem. Soc.* **1993**, *115*, 7772-7777.

[15] A. Demarco, M. Llinas and K. Wuthrich, *Biopolymers* **1978**, *17*, 617-636.

[16] D. Neuhaus and M. P. Williamson, *The Nuclear Overhauser Effect in Structural and Conformational Analysis 2nd Edition*, John Wiley and Sons Ltd, New York, **2000**, p. 656.

[17] C. A. Hunter, *Angew. Chem., Int. Ed* .**2004**, *43*, 5310-5324.

[18] M. S. C. Pedras, N. Ismail, J. W. Quail and S. M. Boyetchko, *Phytochemistry* **2003**, *62*, 1105-1114.

[19] D. Sengupta, R. N. Behera, J. C. Smith and G. M. Ullmann, *Structure* **2005**, *13*, 849-855.

[20] J. W. Quail, N. Ismail, M. S. C. Pedras and S. M. Boyetchko, *Acta Crystallogr., Sect. C: Cryst. Struct. Commun.* **2002**, *58*, o268-o271.

[21] D. Sorensen, T. H. Nielsen, C. Christophersen, J. Sorensen and M. Gajhede, *Acta Crystallogr., Sect. C: Cryst. Struct. Commun.* **2001**, *57*, 1123-1124.

[22] A. Henriksen, U. Anthoni, T. H. Nielsen, J. Sorensen, C. Christophersen and M. Gajhede, *Acta Crystallogr., Sect. C: Cryst. Struct. Commun.* **2000**, *56*, 113-115.

[23] T. Facke and S. Berger, *J. Magn. Reson. Ser. A* **1995**, *113*, 114-116.

[24] J. M. Wieruszeski, I. Landrieu, X. Hanoulle and G. Lippens, *J. Magn. Reson.* **2006**, *181*, 199-202.

[25] S. Akoka, L. Barantin and M. Trierweiler, *Ana.l Chem.* **1999**, *71*, 2554-2557.

[26] A. Jerschow and N. Muller, *J. Magn. Reson.* **1997**, *125*, 372-375.

[27] M. A. Connell, P. J. Bowyer, P. A. Bone, A. L. Davis, A. G. Swanson, M. Nilsson and G. A. Morris, *J. Magn. Reson.* **2009**, *198*, 121-131.

[28] J. S. Alper and R. I. Gelb, *J. Phys. Chem.* **1990**, *94*, 4747-4751.

[29] B. Meyer and T. Peters, *Angew. Chem., Int. Ed.* **2003**, *42*, 864-890.

[30] H. Desvaux and M. Goldman, *J. Magn. Reson. Ser. B* **1996**, *110*, 198-201.

[31] W. F. Vranken, W. Boucher, T. J. Stevens, R. H. Fogh, A. Pajon, P. Llinas, E. L. Ulrich, J. L. Markley, J. Ionides and E. D. Laue, *Proteins: Struct., Funct., Bioinf.* **2005**, *59*, 687-696.

[32] J. R. Maple, U. Dinur and A. T. Hagler, *Proc. Natl. Acad. Sci. U. S. A.* **1988**, *85*, 5350-5354.

Received: ((will be filled in by the editorial staff))
Revised: ((will be filled in by the editorial staff))
Published online: ((will be filled in by the editorial staff))

Entry for the Table of Contents (Please choose one layout only)

Layout 1:

Self-assembling lipodepsipetide

Davy Sinnaeve, Pieter M. S. Hendrickx, Johan Van hemel, Eric Peys, Bruno Kieffer, José C. Martins …….....…… Page – Page

The solution structure and self-association properties of the cyclic lipodepsipeptide pseudodesmin A support its pore forming potential

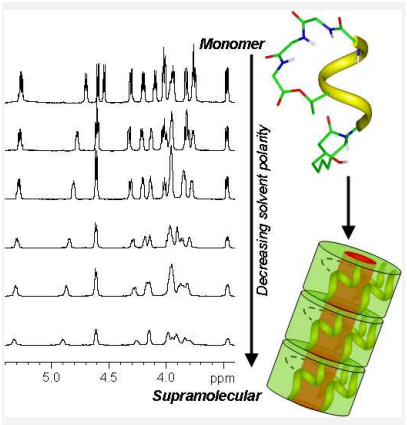

The recently isolated pseudodesmin A forms large supramolecular structures in apolar organic solvents, reminiscent of the ability to form hydrophilic pores in cellular membranes. This is demonstrated by NMR translational diffusion measurements. A model for the supramolecular structure is proposed based on the monomer NMR solution structure and qualitative interpretation of intermolecular contacts.

The solution structure and self-association properties of the cyclic lipodepsipeptide pseudodesmin A support its pore forming potential

Davy Sinnaeve*[a], Pieter M. S. Hendrickx[a], Johan Van hemel[b], Bruno Kieffer[c] and José C. Martins*[a]

[a] *Davy Sinnaeve, Dr. Pieter M. S. Hendrickx, Prof. Dr. José C. Martins*
NMR and Structure Analysis Unit
Department of Organic Chemistry
Ghent University
Krijgslaan 281 S4, B-9000 Gent (Belgium)
Fax: +32 (0)9 264 4972
E-mail: Davy.Sinnaeve@UGent.be, Jose.Martins@UGent.be

[b] *Dr. Johan Van hemel, Dr. Eric Peys*
Kemin Pharma
Atealaan 4H, B-2200 Herentals (Belgium)

[c] *Prof. Dr. Bruno Kieffer*
IGBMC
Biomolecular NMR group
1 rue Laurent Fries BP 10142, 67404 Illkirch CEDEX (France)

Supporting information

Contents:

Additional files:

pseudodesminA_solstruc.pdb: PDB-file containing the lowest energy solution structure

1D ^{1}H NMR spectra of pseudodesmin A in chloroform and DMSO

- p. 4: ca 20 mM solution in chloroform-d, 25°C, 700.13 MHz
- p. 5: solution in DMSO-d6 solution, 298.0 K, 500.13 MHz

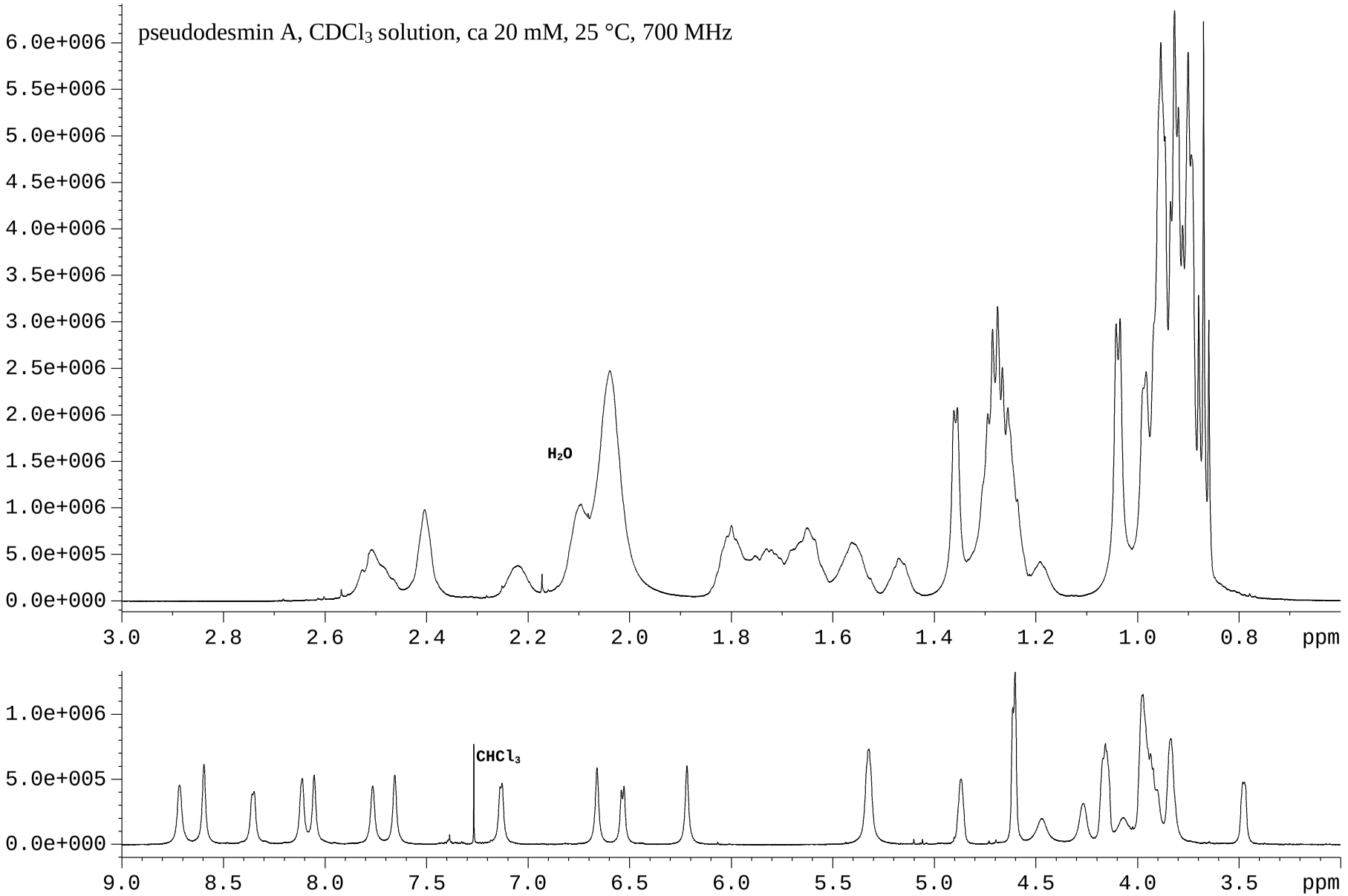
pseudodesmin A, CDCl3 solution, ca 20 mM, 25 °C, 700 MHz
6.0e+006
5.5e+006
5.0e+006
4.5e+006
4.0e+006
3.5e+006
3.0e+006
2.5e+006
2.0e+006
1.5e+006
1.0e+006
5.0e+005
0.0e+000
H2O
3.0
2.8
2.6
2.4
2.2
2.0
1.8
1.6
1.4
1.2
1.0
0.8
ppm
1.0e+006
5.0e+005
0.0e+000
CHCl3
9.0
8.5
8.0
7.5
7.0
6.5
6.0
5.5
5.0
4.5
4.0
3.5
ppm

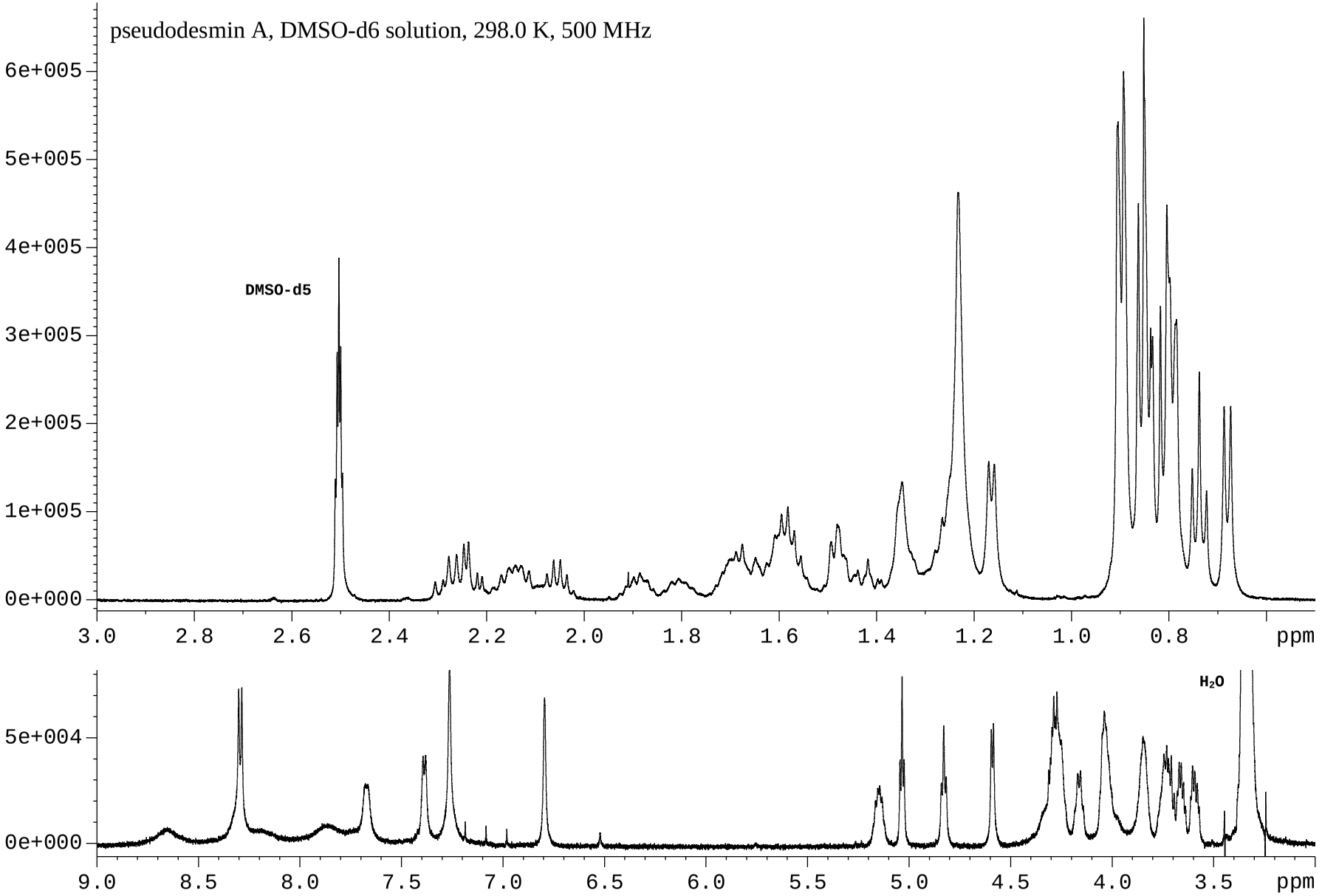
pseudodesmin A, DMSO-d6 solution, 298.0 K, 500 MHz
DMSO-d5
H2O
6e+005
5e+005
4e+005
3e+005
2e+005
1e+005
0e+000
5e+004
0e+000
3.0
2.8
2.6
2.4
2.2
2.0
1.8
1.6
1.4
1.2
1.0
0.8
ppm
9.0
8.5
8.0
7.5
7.0
6.5
6.0
5.5
5.0
4.5
4.0
3.5
ppm

^{1}H, ^{13}C and ^{15}N NMR assignments of pseudodesmin A in DMSO and chloroform solution

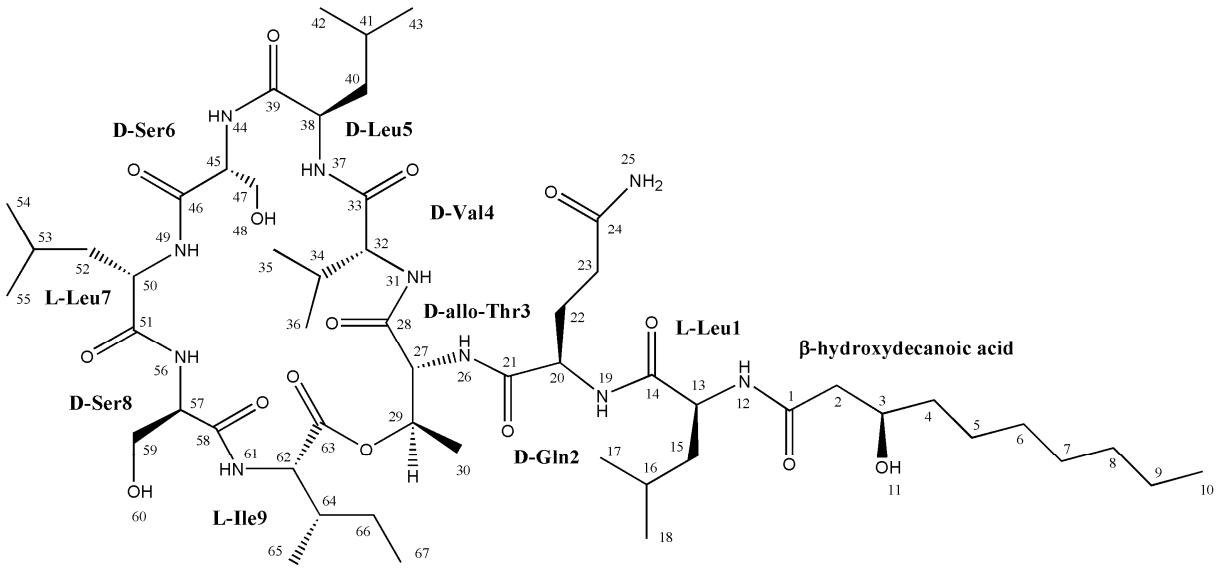

The spectra measured and strategy employed for the ^{1}H, ^{13}C and ^{15}N assignment of pseudodesmin A in DMSO solution were similar as in acetonitrile[1]. The ^{1}H and ^{13}C assignment was performed on a Bruker DRX spectrometer operating at a respective ^{1}H and ^{13}C frequency of 500.13 MHz and 125.76 MHz equipped with a ^{1}H,^{13}C,^{15}N TXI-Z probe. The temperature was set at 298.0 K throughout. The ^{15}N assignment was performed on a Bruker Avance II spectrometer operating at a respective ^{1}H, ^{13}C and ^{15}N frequency of 700.13 MHz and 176.05 MHz and 70.94 MHz also equipped with a ^{1}H,^{13}C,^{15}N TXI-Z probe. The temperature was set at 323.0 K to increase signal to noise by sharpening up the H^{N} resonances.

Assignments in chloroform (ca 20 mM) were performed similarly at 700.13 MHz at 25°C throughout.

In all cases, the ^{1}H and ^{13}C chemical shifts are referenced against internal TMS, while the ^{15}N chemical shift was referenced indirectly to $MeNO_2$ according to IUPAC guidelines[2].

[1] D. Sinnaeve, C. Michaux, J. Van hemel, J. Vandenkerckhove, E. Peys, F. A. M. Borremans, B. Sas, J. Wouters and J. C. Martins, *Tetrahedron* **2009**, *65*, 4173–4181.
[2] R. K. Harris, E. D. Becker, S. M. C. De Menezes, R. Goodfellow and P. Granger, *Pure and Applied Chemistry* **2001**, *73*, 1795-1818.

NMR assignment for pseudodesmin A in DMSO solution*

		^{1}H δ [ppm]	^{13}C δ [ppm]	^{15}N δ [ppm]
HDA				
	CO 1		172.08	
	CH_2α 2	2.27	43.30	
	CHβ 3	3.85	67.41	
	CH_2γ 4	1.36	37.03	
	CH_2δ 5	1.24 / 1.36	24.88	
	CH_2ε 6	1.23	28.79	
	CH_2ζ 7	1.23	28.79	
	CH_2η 8	1.23	31.11	
	CH_2θ 9	1.26	21.96	
	CH_3ι 10	0.85	13.80	
	OH 11	4.59		
Leu1				
	NH 12	8.31		-259.59
	CHα 13	4.14	51.81	
	CO 14		173.41	
	CH_2β 15	1.49	39.82	
	CHγ 16	1.59	24.01	
	CH_3δ 17	0.86	21.89	
	CH_3δ 18	0.90	22.57	
Gln2				
	NH 19	8.65		-253.24
	CHα 20	4.01	54.05	
	CO 21		172.95	
	CH_2β 22	1.83 / 1.90	26.61	
	CH_2γ 23	2.16	31.18	
	COδ 24		173.27	
	NH_2 25	6.79 / 7.26		-272.15
Thr3				
	NH 26	8.29		-267.23
	CHα 27	4.25	58.28	
	CO 28		ND	
	CHβ 29	5.16	68.65	
	CH_3γ 30	1.18	17.27	
Val4				
	NH 31	7.86		-262.11
	CHα 32	3.81	60.27	
	CO 33		170.66	
	CHβ 34	2.06	29.85	
	CH_3γ 35	0.81	19.06	
	CH_3γ 36	0.81	18.47	
Leu5				
	NH 37	7.39		-265.50
	CHα 38	4.28	51.89	
	CO 39		ND	
	CH_2β 40	1.43 / 1.67	39.77	
	CHγ 41	1.70	23.91	
	CH_3δ 42	0.84	20.53	
	CH_3δ 43	0.89	22.94	
Ser6				
	NH 44	8.19		-269.89
	CHα 45	4.07	56.70	
	CO 46		170.04	
	CH_2β 47	3.68 / 3.77	61.27	
	OHγ 48	5.03		
Leu7				
	NH 49	7.75		-260.71
	CHα 50	4.24	50.98	
	CO 51		ND	
	CH_2β 52	1.60	39.35	
	CHγ 53	1.70	23.91	
	CH_3δ 54	0.82	20.80	
	CH_3δ 55	0.90	23.08	
Ser8				
	NH 56	7.67		-270.52
	CHα 57	4.29	56.87	
	CO 58		170.21	
	CH_2β 59	3.59 / 3.72	61.60	
	OHγ 60	4.83		
Ile9				
	NH 61	7.26		-268.77
	CHα 62	ND	ND	
	CO 63		168.88	
	CHβ 64	1.62	35.60	
	CH_3γ 65	0.69	14.84	
	CH_2γ 66	0.90 / 1.27	24.55	
	CH_3δ 67	0.75	11.24	

*^{1}H and ^{13}C assignments performed at 500 MHz at 298.0 K, ^{15}N assignments performed at 700 MHz at 323.0 K
ND = not determined

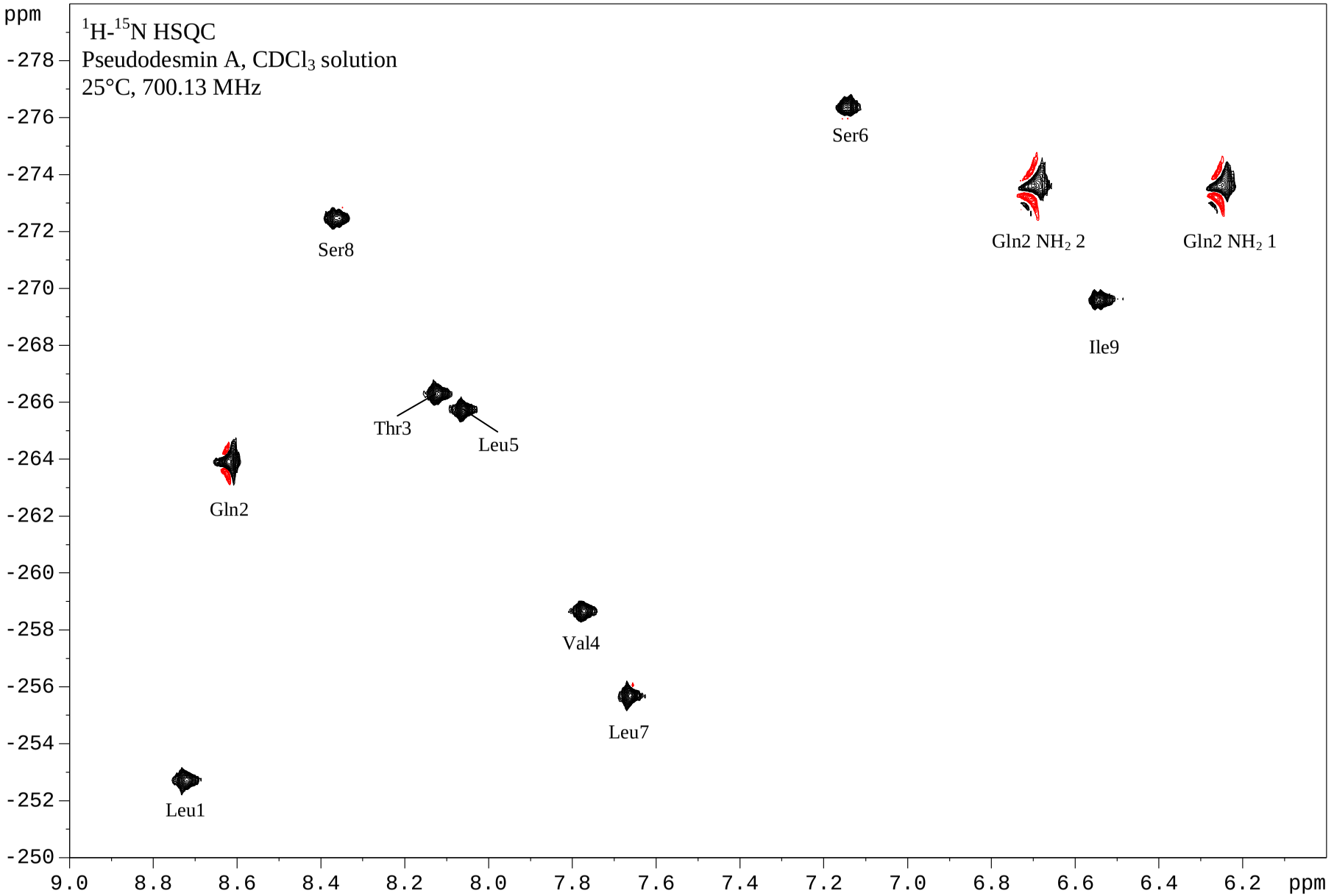
ppm
^{1}H-^{15}N HSQC
Pseudodesmin A, $CDCl_3$ solution
25°C, 700.13 MHz
-278
-276
-274
-272
-270
-268
-266
-264
-262
-260
-258
-256
-254
-252
-250
9.0
8.8
8.6
8.4
8.2
8.0
7.8
7.6
7.4
7.2
7.0
6.8
6.6
6.4
6.2
ppm
Ser6
Gln2 NH_2 2
Gln2 NH_2 1
Ser8
Ile9
Thr3
Leu5
Gln2
Val4
Leu7
Leu1

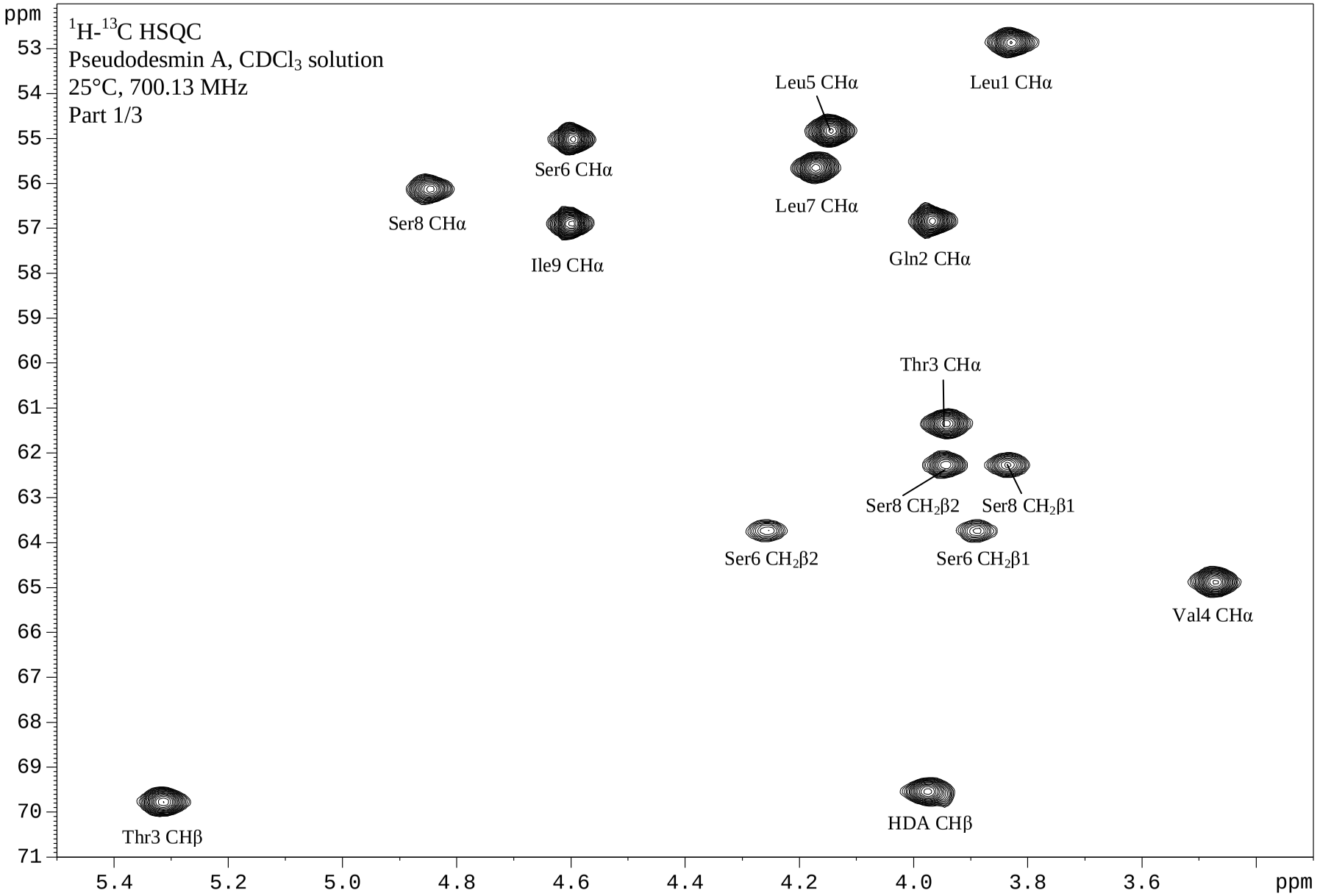
^{1}H-^{13}C HSQC
Pseudodesmin A, $CDCl_3$ solution
25°C, 700.13 MHz
Part 1/3
ppm
53
54
55
56
57
58
59
60
61
62
63
64
65
66
67
68
69
70
71
5.4
5.2
5.0
4.8
4.6
4.4
4.2
4.0
3.8
3.6
ppm
Leu1 CHα
Leu5 CHα
Ser6 CHα
Leu7 CHα
Ser8 CHα
Gln2 CHα
Ile9 CHα
Thr3 CHα
Ser8 CH_2β2
Ser8 CH_2β1
Ser6 CH_2β2
Ser6 CH_2β1
Val4 CHα
Thr3 CHβ
HDA CHβ

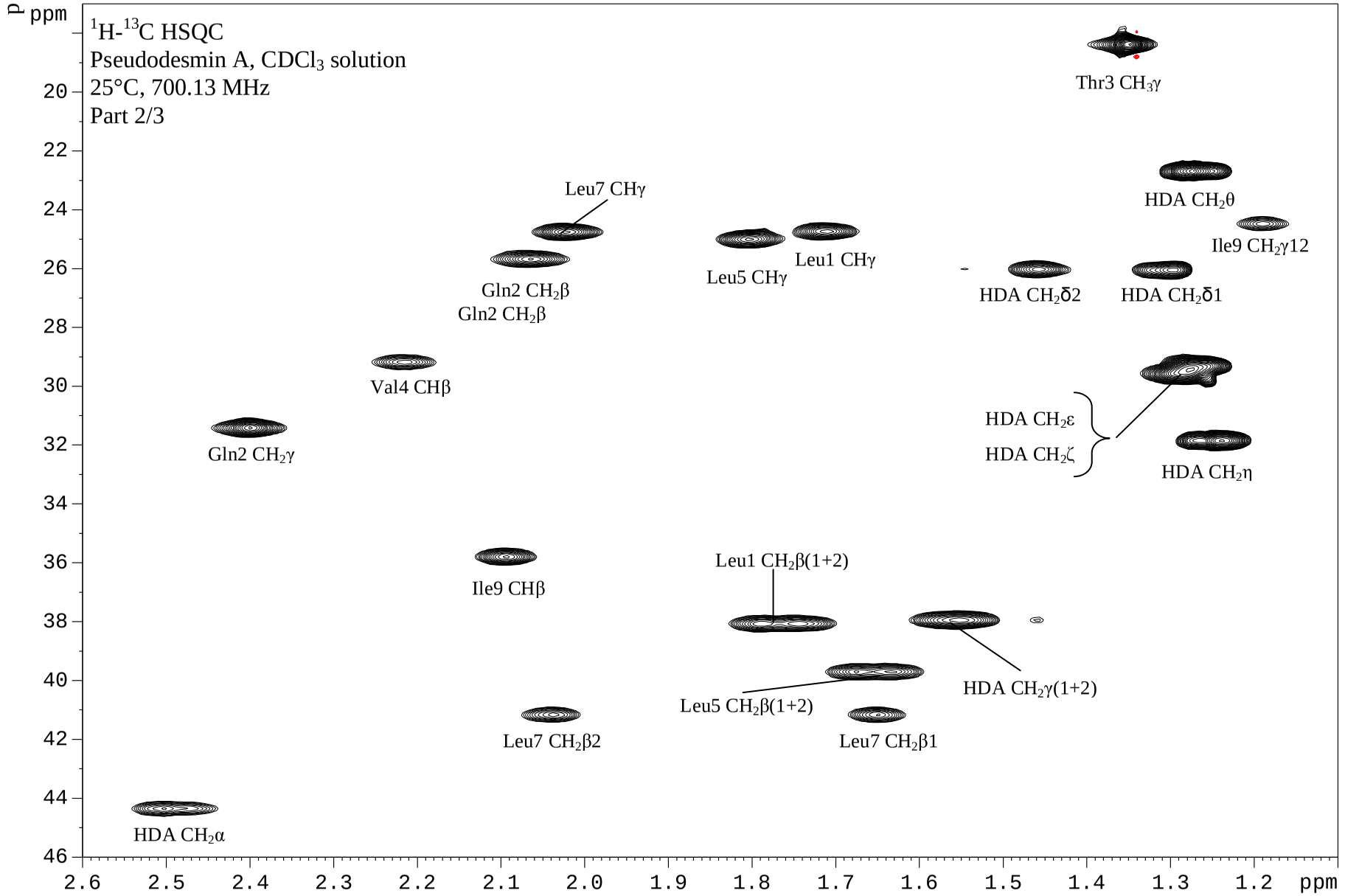
^{1}H-^{13}C HSQC
Pseudodesmin A, $CDCl_3$ solution
25°C, 700.13 MHz
Part 2/3
Thr3 $CH_3\gamma$
HDA $CH_2\theta$
Ile9 $CH_2\gamma12$
Leu7 CHγ
Leu1 CHγ
Leu5 CHγ
Gln2 $CH_2\beta$
Gln2 $CH_2\beta$
HDA $CH_2\delta2$
HDA $CH_2\delta1$
Val4 CHβ
HDA $CH_2\varepsilon$
HDA $CH_2\zeta$
HDA $CH_2\eta$
Gln2 $CH_2\gamma$
Ile9 CHβ
Leu1 $CH_2\beta(1+2)$
HDA $CH_2\gamma(1+2)$
Leu5 $CH_2\beta(1+2)$
Leu7 $CH_2\beta2$
Leu7 $CH_2\beta1$
HDA $CH_2\alpha$
p ppm
20
22
24
26
28
30
32
34
36
38
40
42
44
46
2.6
2.5
2.4
2.3
2.2
2.1
2.0
1.9
1.8
1.7
1.6
1.5
1.4
1.3
1.2
ppm

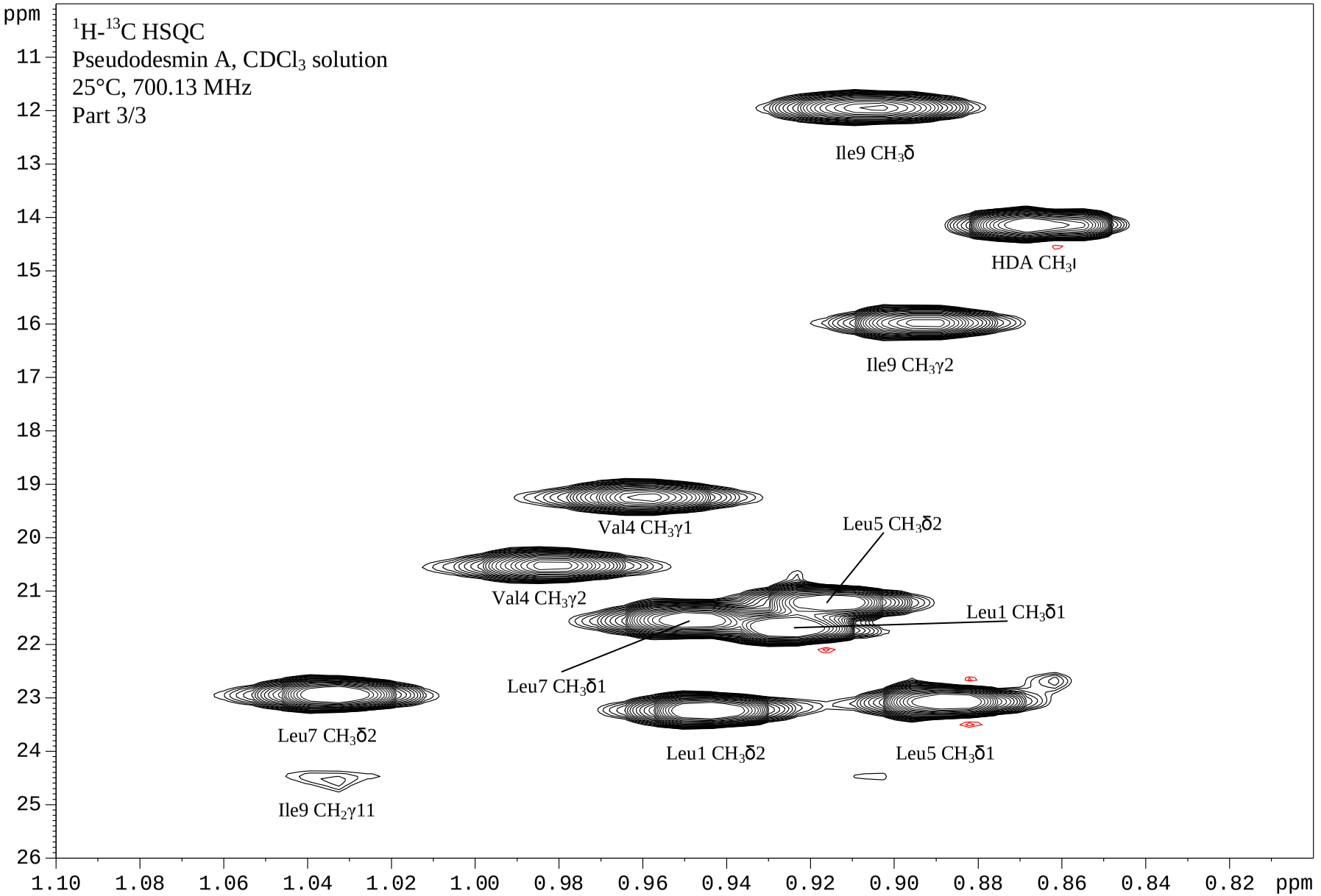
ppm
^{1}H-^{13}C HSQC
Pseudodesmin A, $CDCl_3$ solution
25°C, 700.13 MHz
Part 3/3
Ile9 $CH_3\delta$
HDA CH_3I
Ile9 $CH_3\gamma2$
Val4 $CH_3\gamma1$
Leu5 $CH_3\delta2$
Val4 $CH_3\gamma2$
Leu1 $CH_3\delta1$
Leu7 $CH_3\delta1$
Leu7 $CH_3\delta2$
Leu1 $CH_3\delta2$
Leu5 $CH_3\delta1$
Ile9 $CH_2\gamma11$
11 12 13 14 15 16 17 18 19 20 21 22 23 24 25 26
1.10 1.08 1.06 1.04 1.02 1.00 0.98 0.96 0.94 0.92 0.90 0.88 0.86 0.84 0.82 ppm

2D ^{1}H-^{1}H NOESY spectra 200 ms mixing time in acetonitrile and chloroform and 2D ^{1}H-^{1}H ROESY spectrum 40 ms mixing time in chloroform

A comparison between the 2D ^{1}H-^{1}H NOESY spectra (mixing time 200 ms, measured at 500 MHz) of pseudodesmin A in respectively acetonitrile and chloroform solution illustrates the size of the supramolecular complexes that can be formed in chloroform. In acetonitrile, the product behaves as a small molecule, with clear positive nOe correlations between resonances. In a ca 25mM chloroform solution however, the nOe correlations become strongly negative while spin diffusion is abundantly present, effectively creating a cross-peak between almost every pair of resonances. This effect is due to the strong dependence of the nOe with the rotational correlation time of molecules in solution.

2D ^{1}H-^{1}H ROESY spectra are much less prone to spin diffusion, while any relayed rOe correlations that do get through will experience an inversion of sign and thus be easily recognized. For this reason, a 2D ROESY spectrum (mixing time 40 ms, measured at 700 MHz) of a ca 20 mM pseudodesmin A solution in chloroform was recorded for the detection of intermolecular contacts.

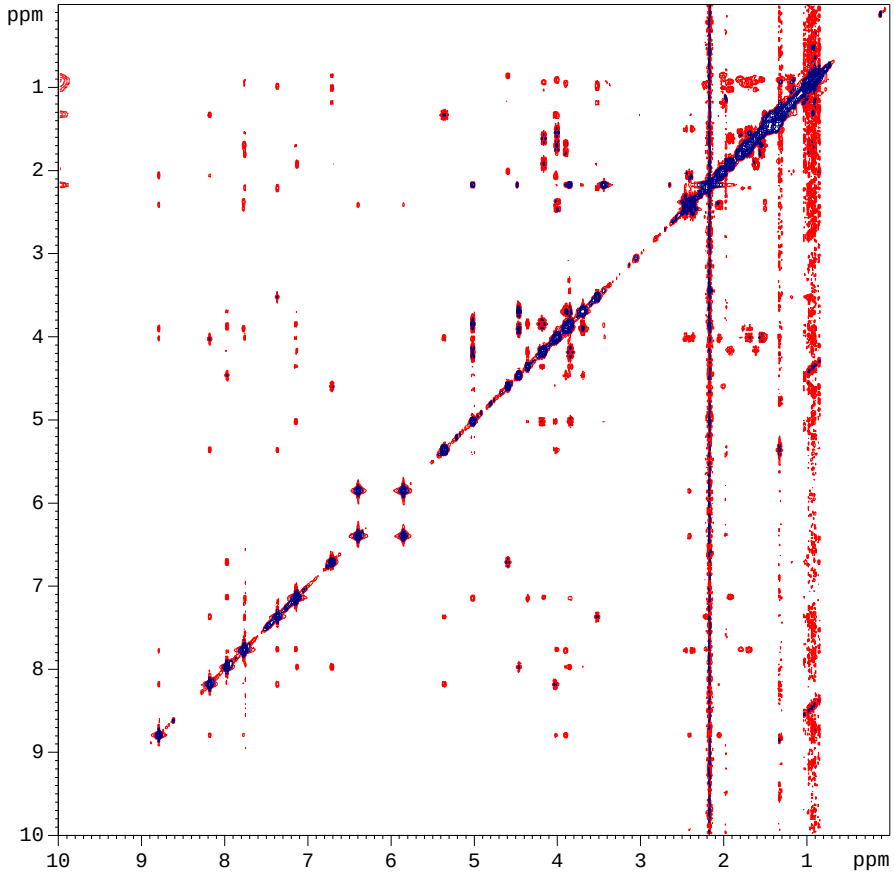

2D NOESY, acetonitrile, 200 ms mixing time

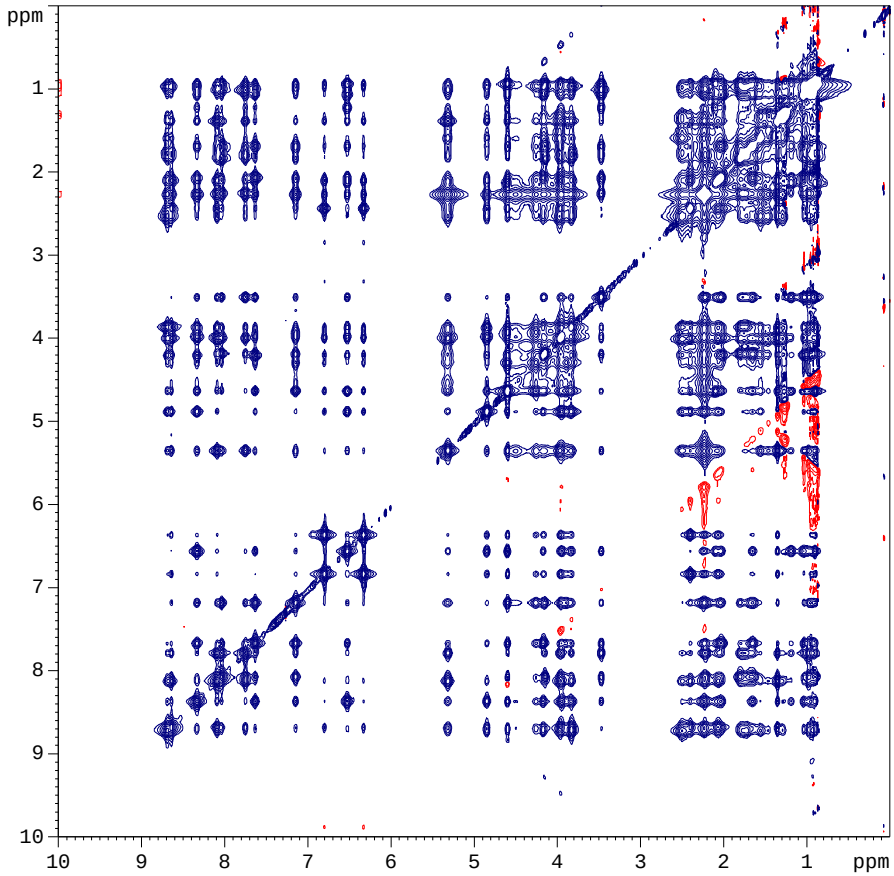

2D NOESY, chloroform, 200 ms mixing time

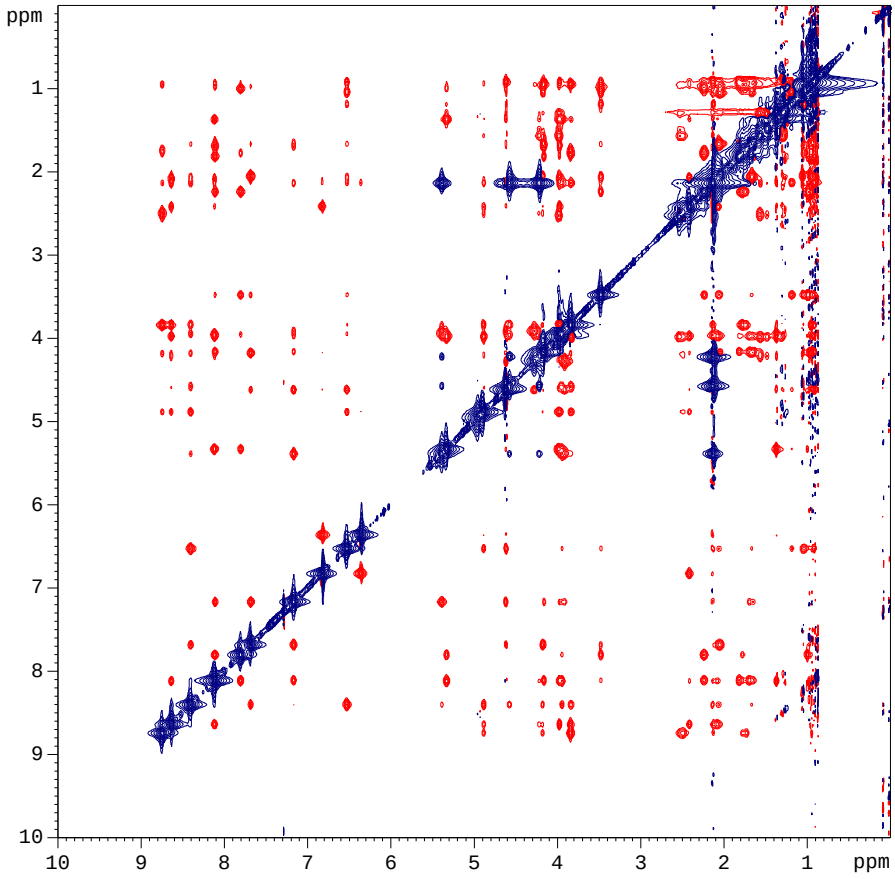

2D off-resonance ROESY, chloroform, 40 ms mixing time

Additional data from solvent titrations

Tabulated data for first titration performed to assess the effect of solvent polarity (see Figure 3 in the main paper)

	pseudodesmin A		TMS	
V% CD_3CN	D [µm²/s]	error[a]	D [µm²/s]	error[a]
0.0	262.3	1.8	1949.5	16.9
1.0	289.2	2.4	1978.7	13.6
2.0	316.5	1.7	1965.1	15.2
3.0	344.5	2.1	1974.4	12.6
4.0	376.8	2.0	1974.0	16.9
5.0	398.2	1.6	1967.8	10.2
6.0	420.3	2.8	1967.2	10.9
7.0	435.7	2.2	1943.2	11.6
8.0	450.8	2.9	1949.7	14.9
9.0	456.8	2.6	1931.2	14.9
10.0	463.0	1.8	1933.5	14.6
11.0	470.1	2.0	1949.3	12.2
12.0	475.6	2.2	1954.3	9.6
13.0	484.7	2.8	1963.6	16.1

[a] 95% error calculated as 1.96 times the standard deviation of 500 diffusion coefficients obtained using a Monte Carlo procedure

Tabulated data for second titration performed to assess the ^1H, ^{13}C and ^{15}N chemical shift changes (see Figure 6 in the main paper)

point			1	2	3	4	5	6	7	8	9	10	11				
			Diffusion coefficients [µm²/s]											ΔD			
$D_{pseudodesmin\ A}$			178.5	202.7	222.1	239.6	265.4	299.3	327.9	348.7	373.4	405.7	436.3	257.8			
error[a]			0.7	1.0	1.4	0.8	1.8	1.6	1.2	1.5	1.7	2.0	2.1				
D_{TMS}			1880.8	1885.5	1862.6	1862.6	1861.3	1857.2	1849.1	1843.4	1859.3	1825.5	1858.9				
error[a]			4.9	10.3	2.9	5.1	2.5	4.2	4.3	3.5	13.0	3.2	3.1				
			$^1H/^{13}C$ Chemical shifts [ppm]											Slope[b]	R^2	|Slope|×ΔD	average[c]
Leu1	CHα	^1H	3.84	3.83	3.82	3.81	3.80	3.79	3.78	3.77	3.77	3.77	3.77	-2.95E-04	-0.96	0.08	0.23
		^{13}C	52.74	52.80	52.82	52.84	52.90	52.94	52.96	52.98	53.02	53.04	53.05	1.21E-03	0.99	0.31	
Leu1	$CH_2\beta(1+2)$	^1H	1.77	1.77	1.77	1.77	1.77	1.76	1.76	1.75	1.75	1.74	1.73	-1.54E-04	-0.99	0.04	0.13
		^{13}C	37.88	37.90	37.89	37.90	37.91	37.93	37.94	37.96	37.97	38.02	38.08	6.65E-04	0.94	0.17	
Leu1	CHγ	^1H	1.72	1.72	1.71	1.71	1.70	1.69	1.68	1.68	1.67	1.67	1.66	-2.52E-04	-1.00	0.06	0.08
		^{13}C	24.61	24.62	24.61	24.61	24.61	24.62	24.61	24.62	24.62	24.64	24.66	1.19E-04	0.74	0.03	
Leu1	$CH_3\delta1$	^1H	0.94	0.93	0.93	0.93	0.93	0.93	0.93	0.92	0.92	0.92	0.92	-8.33E-05	-0.98	0.02	0.03
		^{13}C	21.53	21.55	21.54	21.53	21.53	21.54	21.53	21.53	21.54	21.53	21.57	4.98E-05	0.38	0.01	
Leu1	$CH_3\delta2$	^1H	0.95	0.95	0.95	0.95	0.95	0.95	0.95	0.95	0.95	0.95	0.95	-5.60E-06	-0.53	0.00	0.09
		^{13}C	23.26	23.23	23.20	23.18	23.18	23.18	23.14	23.12	23.12	23.08	23.08	-6.64E-04	-0.97	0.17	
Gln2	CHα	^1H	3.99	3.98	3.98	3.98	3.97	3.97	3.96	3.96	3.96	3.95	3.94	-1.73E-04	-1.00	0.04	0.11
		^{13}C	56.61	56.63	56.64	56.60	56.63	56.64	56.65	56.67	56.67	56.72	56.77	5.13E-04	0.87	0.13	
Gln2	$CH_2\beta$	^1H	2.07	2.08	2.07	2.07	2.07	2.07	2.07	2.07	2.06	2.06	2.05	-9.00E-05	-0.93	0.02	0.23
		^{13}C	25.65	25.56	25.50	25.46	25.39	25.32	25.26	25.24	25.19	25.21	25.29	-1.63E-03	-0.90	0.42	
Gln2	$CH_2\gamma$	^1H	2.41	2.42	2.42	2.42	2.43	2.43	2.43	2.43	2.43	2.43	2.42	4.77E-05	0.54	0.01	0.11
		^{13}C	31.21	31.26	31.27	31.25	31.29	31.32	31.32	31.36	31.36	31.40	31.44	7.78E-04	0.98	0.20	
Thr3	CHα	^1H	3.92	3.94	3.96	3.97	3.99	4.01	4.02	4.03	4.04	4.03	4.02	4.36E-04	0.92	0.11	0.49
		^{13}C	61.38	61.24	61.13	61.08	60.95	60.83	60.74	60.70	60.64	60.62	60.67	-2.95E-03	-0.95	0.76	
Thr3	CHβ	^1H	5.32	5.31	5.31	5.30	5.30	5.29	5.28	5.27	5.27	5.27	5.26	-2.35E-04	-0.99	0.06	0.17
		^{13}C	69.71	69.69	69.66	69.65	69.64	69.61	69.57	69.56	69.52	69.51	69.52	-8.24E-04	-0.98	0.21	
Thr3	$CH_3\gamma$	^1H	1.36	1.35	1.35	1.34	1.34	1.34	1.33	1.33	1.32	1.32	1.31	-1.56E-04	-0.99	0.04	0.21
		^{13}C	18.38	18.29	18.23	18.19	18.19	18.14	18.08	18.04	18.03	18.00	18.05	-1.35E-03	-0.94	0.35	
Val4	CHα	^1H	3.47	3.47	3.48	3.47	3.47	3.47	3.48	3.47	3.48	3.48	3.47	1.34E-05	0.56	0.00	0.21
		^{13}C	64.84	64.78	64.72	64.69	64.63	64.58	64.52	64.51	64.46	64.45	64.46	-1.57E-03	-0.97	0.41	
Val4	CHβ	^1H	2.22	2.21	2.21	2.20	2.20	2.19	2.18	2.18	2.17	2.17	2.17	-1.99E-04	-0.98	0.05	0.05
		^{13}C	29.13	29.14	29.14	29.12	29.13	29.13	29.12	29.13	29.13	29.13	29.15	2.66E-05	0.28	0.01	
Val4	$CH_3\gamma1$	^1H	0.97	0.97	0.97	0.97	0.97	0.97	0.97	0.97	0.97	0.97	0.96	-1.35E-05	-0.48	0.00	0.02
		^{13}C	19.24	19.23	19.22	19.22	19.22	19.24	19.25	19.23	19.25	19.25	19.28	1.44E-04	0.70	0.04	
Val4	$CH_3\gamma2$	^1H	0.99	0.98	0.98	0.98	0.98	0.98	0.98	0.98	0.97	0.97	0.97	-6.79E-05	-0.97	0.02	0.11
		^{13}C	20.44	20.47	20.47	20.48	20.48	20.51	20.54	20.54	20.58	20.58	20.64	7.20E-04	0.98	0.19	

Leu5	CHα	^{1}H	4.15	4.15	4.14	4.15	4.14	4.14	4.14	4.13	4.13	4.12	4.10	-1.45E-04	-0.86	0.04	0.13
		^{13}C	54.79	54.73	54.68	54.65	54.62	54.58	54.55	54.55	54.53	54.56	54.64	-7.18E-04	-0.76	0.19	
Leu5	CH_2β(1+2)	^{1}H	1.65	1.65	1.65	1.65	1.64	1.64	1.64	1.64	1.64	1.63	1.62	-9.25E-05	-0.98	0.02	0.16
		^{13}C	39.63	39.66	39.65	39.67	39.71	39.75	39.77	39.80	39.82	39.86	39.91	1.08E-03	0.99	0.28	
Leu5	CHγ	^{1}H	1.80	1.80	1.80	1.80	1.80	1.79	1.79	1.79	1.79	1.79	1.78	-7.19E-05	-0.99	0.02	0.06
		^{13}C	24.94	24.93	24.90	24.89	24.90	24.90	24.87	24.87	24.86	24.86	24.87	-2.91E-04	-0.90	0.08	
Leu5	CH_3δ1	^{1}H	0.90	0.89	0.89	0.89	0.89	0.88	0.88	0.88	0.87	0.87	0.87	-9.51E-05	-0.98	0.02	0.06
		^{13}C	23.00	23.02	23.02	23.02	23.02	23.05	23.06	23.05	23.07	23.07	23.07	2.81E-04	0.97	0.07	
Leu5	CH_3δ2	^{1}H	0.92	0.92	0.92	0.92	0.92	0.92	0.91	0.91	0.91	0.91	0.90	-7.45E-05	-0.99	0.02	0.05
		^{13}C	21.22	21.19	21.17	21.15	21.15	21.16	21.13	21.11	21.14	21.11	21.16	-2.76E-04	-0.71	0.07	
Ser6	CHα	^{1}H	4.61	4.61	4.61	4.61	4.61	4.61	4.61	4.60	4.60	4.57	4.54	-2.10E-04	-0.77	0.05	0.07
		^{13}C	54.86	54.82	54.80	54.78	54.76	54.76	54.75	54.77	54.77	54.83	54.94	1.28E-04	0.19	0.03	
Ser6	CH_2β1	^{1}H	3.90	3.89	3.89	3.87	3.86	3.85	3.84	3.83	3.83	3.83	3.83	-3.13E-04	-0.96	0.08	0.26
		^{13}C	63.73	63.78	63.82	63.84	63.91	63.95	63.98	64.01	64.04	64.06	64.09	1.40E-03	0.99	0.36	
Ser6	CH_2β2	^{1}H	4.26	4.27	4.28	4.28	4.29	4.30	4.31	4.32	4.32	4.32	4.31	2.23E-04	0.91	0.06	0.24
		^{13}C	63.70	63.79	63.81	63.85	63.90	63.96	63.98	64.01	64.04	64.07	64.09	1.45E-03	0.98	0.37	
Leu7	CHα	^{1}H	4.15	4.17	4.18	4.18	4.19	4.20	4.21	4.21	4.21	4.21	4.20	2.16E-04	0.89	0.06	0.60
		^{13}C	55.86	55.70	55.58	55.52	55.40	55.25	55.13	55.05	54.95	54.84	54.75	-4.24E-03	-1.00	1.09	
Leu7	CH_2β1	^{1}H	1.66	1.66	1.66	1.66	1.66	1.66	1.66	1.66	1.66	1.65	1.65	-2.41E-05	-0.62	0.01	0.15
		^{13}C	41.04	41.09	41.12	41.12	41.17	41.21	41.23	41.26	41.27	41.31	41.33	1.09E-03	0.99	0.28	
Leu7	CH_2β2	^{1}H	2.06	2.04	2.03	2.03	2.01	1.99	1.98	1.97	1.96	1.95	1.94	-4.70E-04	-0.99	0.12	0.26
		^{13}C	41.06	41.11	41.12	41.14	41.18	41.21	41.23	41.27	41.28	41.31	41.34	1.05E-03	1.00	0.27	
Leu7	CHγ	^{1}H	2.03	2.03	2.03	2.03	2.03	2.03	2.03	2.02	2.02	2.02	2.01	-5.89E-05	-0.76	0.02	0.03
		^{13}C	24.68	24.67	24.66	24.66	24.66	24.66	24.65	24.66	24.67	24.69	24.73	1.26E-04	0.49	0.03	
Leu7	CH_3δ1	^{1}H		0.95	0.95	0.95	0.95	0.95	0.95	0.95	0.95	0.95	0.94	-3.04E-05	-0.81	0.01	0.09
		^{13}C		21.49	21.45	21.44	21.44	21.42	21.39	21.36	21.36	21.34	21.33	-6.57E-04	-0.98	0.17	
Leu7	CH_3δ2	^{1}H	1.04	1.04	1.04	1.04	1.04	1.04	1.03	1.03	1.03	1.03	1.02	-5.81E-05	-0.96	0.01	0.13
		^{13}C	22.90	22.93	22.93	22.95	22.95	22.99	23.02	23.04	23.07	23.08	23.15	9.13E-04	0.98	0.24	
Ser8	CHα	^{1}H	4.89	4.88	4.86	4.85	4.83	4.82	4.80	4.79	4.77	4.74	4.69	-7.16E-04	-0.99	0.18	0.51
		^{13}C	56.13	56.04	55.96	55.94	55.85	55.75	55.66	55.59	55.54	55.50	55.54	-2.56E-03	-0.98	0.66	
Ser8	CH_2β1	^{1}H	3.81	3.84	3.86	3.87	3.90	3.94	3.97	3.98	4.01	4.02	4.02	8.80E-04	0.98	0.23	0.47
		^{13}C	62.15	62.18	62.19	62.23	62.27	62.34	62.38	62.45	62.49	62.57	62.61	1.88E-03	1.00	0.48	
Ser8	CH_2β2	^{1}H	3.98	3.96	3.93	3.93	3.90	3.88	3.85	3.83	3.81	3.78	3.76	-8.79E-04	-1.00	0.23	0.47
		^{13}C	62.16	62.20	62.20	62.21	62.27	62.35	62.39	62.46	62.49	62.57	62.62	1.86E-03	0.99	0.48	
Ile9	CHα	^{1}H	4.61	4.61	4.60	4.61	4.61	4.61	4.61	4.61	4.61	4.60	4.60	-3.01E-05	-0.56	0.01	0.16
		^{13}C	56.87	56.83	56.79	56.78	56.75	56.71	56.66	56.65	56.61	56.59	56.58	-1.16E-03	-0.99	0.30	
Ile9	CHβ	^{1}H	2.12	2.11	2.10	2.10	2.09	2.09	2.08	2.07	2.07	2.06	2.05	-2.62E-04	-1.00	0.07	0.20
		^{13}C	35.59	35.62	35.63	35.62	35.65	35.68	35.71	35.74	35.76	35.81	35.88	1.04E-03	0.98	0.27	
Ile9	CH_2γ11	^{1}H	1.03	1.03	1.03	1.03	1.03	1.04	1.04	1.04	1.04	1.04	1.03	3.54E-05	0.49	0.01	0.06
		^{13}C	24.35	24.36	24.36	24.34	24.37	24.39	24.37	24.39	24.39	24.43	24.45	3.72E-04	0.91	0.10	
Ile9	CH_2γ12	^{1}H	1.18	1.18	1.17	1.17	1.17	1.17	1.16	1.16	1.16	1.16	1.16	-8.80E-05	-0.96	0.02	0.07
		^{13}C	24.36	24.37	24.36	24.35	24.37	24.38	24.38	24.39	24.40	24.43	24.45	3.43E-04	0.92	0.09	
Ile9	CH_3γ2	^{1}H	0.90	0.90	0.90	0.90	0.90	0.90	0.90	0.89	0.89	0.89	0.88	-6.90E-05	-0.90	0.02	0.02
		^{13}C	15.96	15.96	15.94	15.94	15.94	15.95	15.95	15.93	15.95	15.94	15.96	3.85E-06	0.03	0.00	
Ile9	CH_3δ	^{1}H	0.91	0.91	0.91	0.91	0.91	0.90	0.90	0.90	0.90	0.89	0.89	-8.92E-05	-0.99	0.02	0.06
		^{13}C	11.94	11.94	11.93	11.93	11.93	11.95	11.96	11.96	11.98	11.97	12.02	2.85E-04	0.87	0.07	
HDA	CH_2α1	^{1}H	2.51	2.51	2.46	2.46	2.43	2.42	2.40	2.39	2.38	2.36	2.35	-6.50E-04	-0.98	0.17	0.31
		^{13}C	44.45	44.43	44.39	44.40	44.37	44.34	44.29	44.27	44.25	44.20	44.17	-1.07E-03	-0.99	0.28	
HDA	CH_2α2	^{1}H	2.51	2.51	2.50	2.50	2.50	2.49	2.48	2.48	2.47	2.47	2.46	-2.16E-04	-1.00	0.06	0.19
		^{13}C	44.45	44.43	44.39	44.38	44.37	44.33	44.30	44.27	44.25	44.20	44.16	-1.07E-03	-1.00	0.28	
HDA	CHβ	^{1}H	3.95	3.95	3.96	3.96	3.96	3.96	3.96	3.96	3.96	3.96	3.96	4.71E-05	0.96	0.01	0.34
		^{13}C	69.58	69.45	69.37	69.31	69.23	69.14	69.06	69.04	68.98	68.94	68.93	-2.51E-03	-0.97	0.65	
HDA	CH_2γ	^{1}H	1.56	1.55	1.55	1.55	1.54	1.54	1.53	1.53	1.53	1.52	1.51	-1.53E-04	-1.00	0.04	0.13
		^{13}C	38.03	37.99	37.96	37.94	37.94	37.91	37.89	37.88	37.86	37.85	37.83	-7.02E-04	-0.98	0.18	
HDA	CH_2δ1	^{1}H	1.29	1.30	1.30	1.30	1.30	1.30	1.30	1.30	1.30	1.30	1.30	1.40E-05	0.74	0.00	0.21
		^{13}C	26.07	26.01	25.95	25.92	25.88	25.82	25.76	25.75	25.70	25.68	25.69	-1.56E-03	-0.97	0.40	
HDA	CH_2δ2	^{1}H	1.47	1.47	1.47	1.46	1.46	1.45	1.45	1.45	1.44	1.44	1.43	-1.52E-04	-1.00	0.04	0.24
		^{13}C	26.05	25.98	25.94	25.92	25.87	25.80	25.74	25.72	25.68	25.65	25.67	-1.59E-03	-0.98	0.41	
HDA	CH_2θ	^{1}H	1.27	1.27	1.28	1.28	1.28	1.28	1.28	1.28	1.28	1.29	1.29	5.29E-05	0.97	0.01	0.06
		^{13}C	22.66	22.65	22.64	22.64	22.67	22.66	22.66	22.69	22.68	22.71	22.76	3.50E-04	0.84	0.09	
HDA	CH_3ι	^{1}H	0.87	0.87	0.87	0.87	0.87	0.87	0.88	0.88	0.88	0.88	0.88	4.73E-05	0.99	0.01	0.03
		^{13}C	14.14	14.13	14.12	14.12	14.12	14.14	14.14	14.14	14.15	14.14	14.18	1.59E-04	0.72	0.04	
						^{1}H/^{15}N Chemical shifts [ppm]								Slope[b]	R^2	|Slope|×ΔD	average[c]
Leu1	NH	^{1}H		8.54	8.47	8.41	8.31	8.19	8.11	8.05	7.96	7.89	7.86	-3.04E-03	-0.99	0.78	1.12
		^{15}N		-253.08	-253.19	-253.35	-253.71	-253.95	-254.19	-254.27	-254.45	-254.49	-254.39	-6.46E-03	-0.95	1.67	
Gln2	NH	^{1}H			8.73	8.78	8.87	8.94	9.00	9.03	9.08	9.10	9.08	1.74E-03	0.95	0.45	0.75
		^{15}N			-263.58	-263.53	-263.31	-263.14	-263.00	-262.90	-262.73	-262.55	-262.32	5.79E-03	1.00	1.49	
Thr3	NH	^{1}H	8.12	8.11	8.11	8.11	8.11	8.11	8.11	8.11	8.11	8.11	8.13	1.07E-05	0.15	0.00	0.03
		^{15}N	-266.15	-266.17	-266.13	-266.13	-266.09	-266.08	-266.07	-266.05	-266.04	-266.05	-266.04	5.01E-04	0.94	0.13	
Val4	NH	^{1}H	7.78	7.72	7.68	7.64	7.58	7.52	7.47	7.44	7.39	7.36	7.35	-1.74E-03	-0.99	0.45	0.67
		^{15}N	-258.56	-258.79	-258.88	-258.97	-259.09	-259.23	-259.35	-259.46	-259.55	-259.64	-259.64	-4.20E-03	-0.98	1.08	
Leu5	NH	^{1}H	8.08	8.04	8.01	7.98	7.92	7.88	7.84	7.81	7.78	7.76	7.76	-1.33E-03	-0.98	0.34	0.55
		^{15}N	-265.65	-265.79	-265.91	-265.97	-266.18	-266.33	-266.44	-266.52	-266.61	-266.64	-266.60	-4.05E-03	-0.97	1.04	

Ser6	NH	^{1}H	7.14	7.12	7.11	7.10	7.09	7.06	7.06	7.05	7.04	7.03	7.04	-4.07E-04	-0.96	0.10	0.13
		^{15}N	-276.52	-276.57	-276.53	-276.59	-276.58	-276.57	-276.56	-276.58	-276.64	-276.64	-276.69	-4.79E-04	-0.85	0.12	
Leu7	NH	^{1}H	7.70	7.64	7.60	7.58	7.52	7.46	7.42	7.39	7.35	7.31	7.28	-1.64E-03	-1.00	0.42	1.06
		^{15}N	-255.34	-255.76	-256.04	-256.22	-256.62	-256.98	-257.32	-257.59	-257.86	-258.24	-258.58	-1.23E-02	-1.00	3.17	
Ser8	NH	^{1}H	8.43	8.38	8.36	8.34	8.30	8.27	8.24	8.21	8.19	8.15	8.12	-1.14E-03	-1.00	0.30	0.76
		^{15}N	-272.52	-272.73	-272.88	-273.03	-273.30	-273.64	-273.88	-274.13	-274.35	-274.62	-274.71	-9.04E-03	-1.00	2.33	
Ile9	NH	^{1}H	6.48	6.50	6.50	6.49	6.49	6.50	6.50	6.51	6.51	6.52	6.54	1.61E-04	0.91	0.04	0.07
		^{15}N	-269.99	-270.07	-270.06	-270.15	-270.19	-270.17	-270.19	-270.19	-270.20	-270.19	-270.16	-6.09E-04	-0.76	0.16	

[a] 95% error calculated as 1.96 times the standard deviation of 500 diffusion coefficients obtained using a Monte Carlo procedure
[b] Slope obtained by linear regression between chemical shift and pseudodesmin A diffusion coefficients
[c] Average chemical shift change calculated as $\delta_{av} = \delta(^{1}H) + \delta(X)/n$ with n=2 for X=^{13}C and n=5 for X=^{15}N

<u>Second titration 1D ^{1}H spectra: evolution of chemical shift and line width</u>

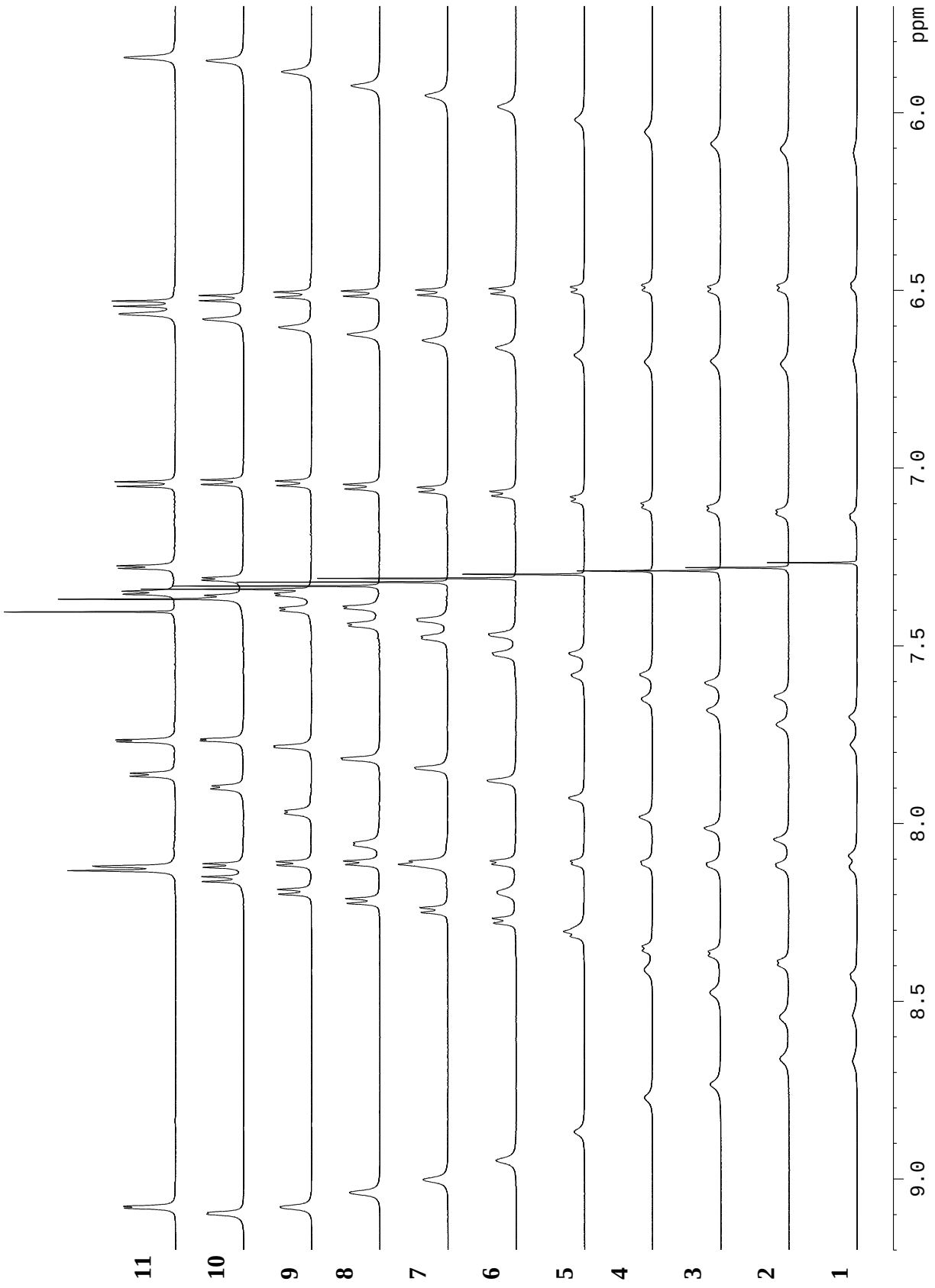
11
10
9
8
7
6
5
4
3
2
1
9.0
8.5
8.0
7.5
7.0
6.5
6.0
ppm

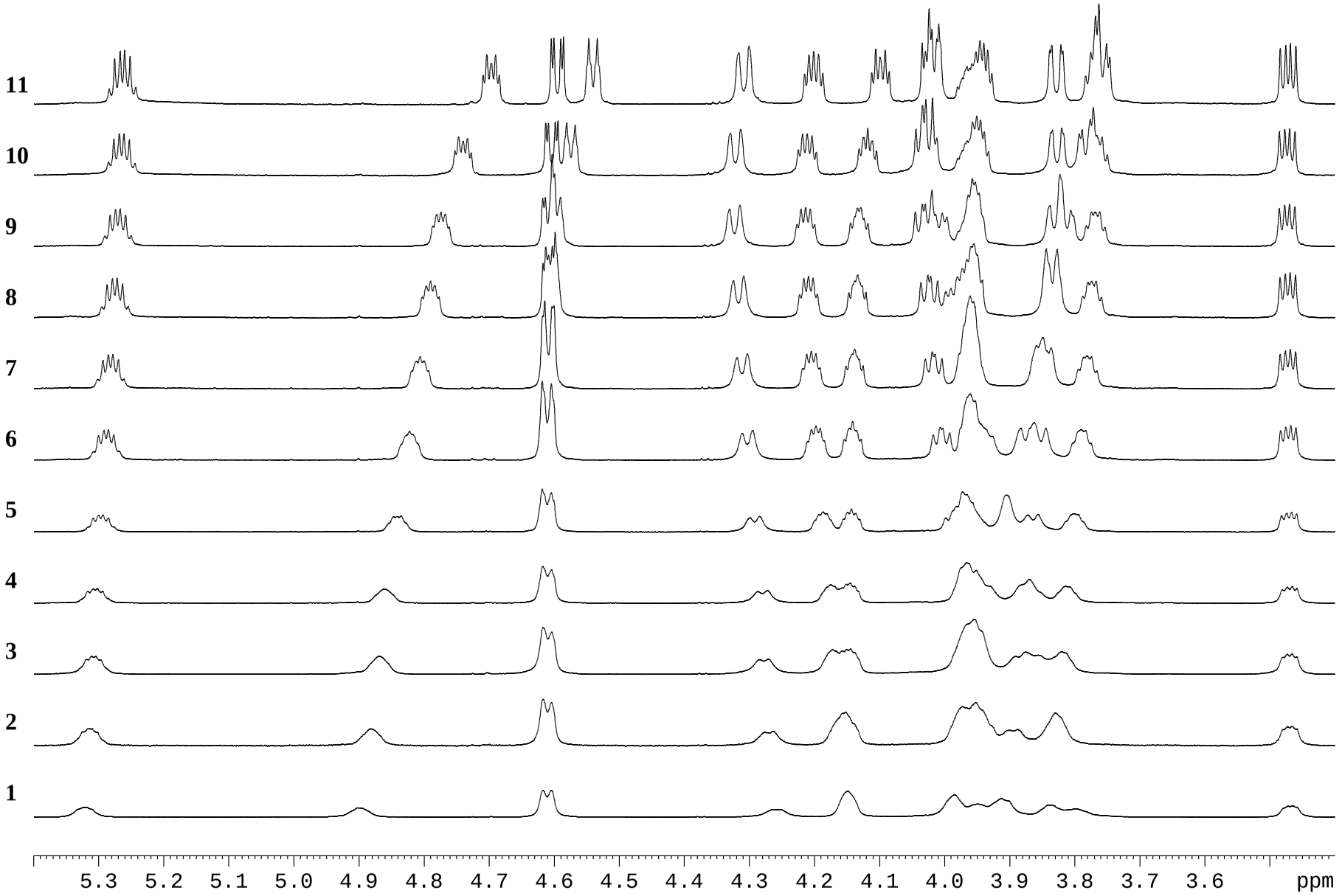
11
10
9
8
7
6
5
4
3
2
1
5.3 5.2 5.1 5.0 4.9 4.8 4.7 4.6 4.5 4.4 4.3 4.2 4.1 4.0 3.9 3.8 3.7 3.6
ppm

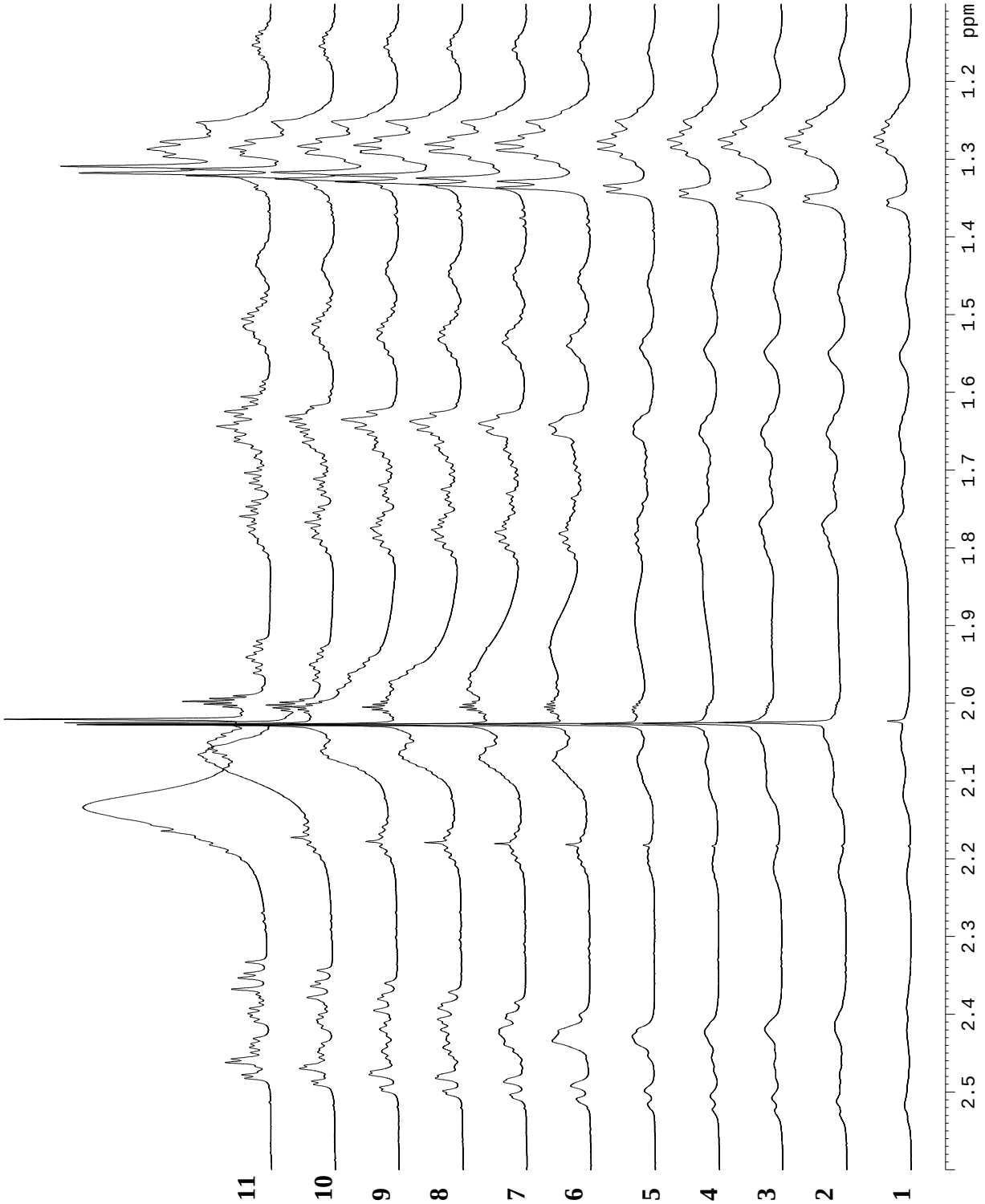
11
10
9
8
7
6
5
4
3
2
1
2.5
2.4
2.3
2.2
2.1
2.0
1.9
1.8
1.7
1.6
1.5
1.4
1.3
1.2
ppm

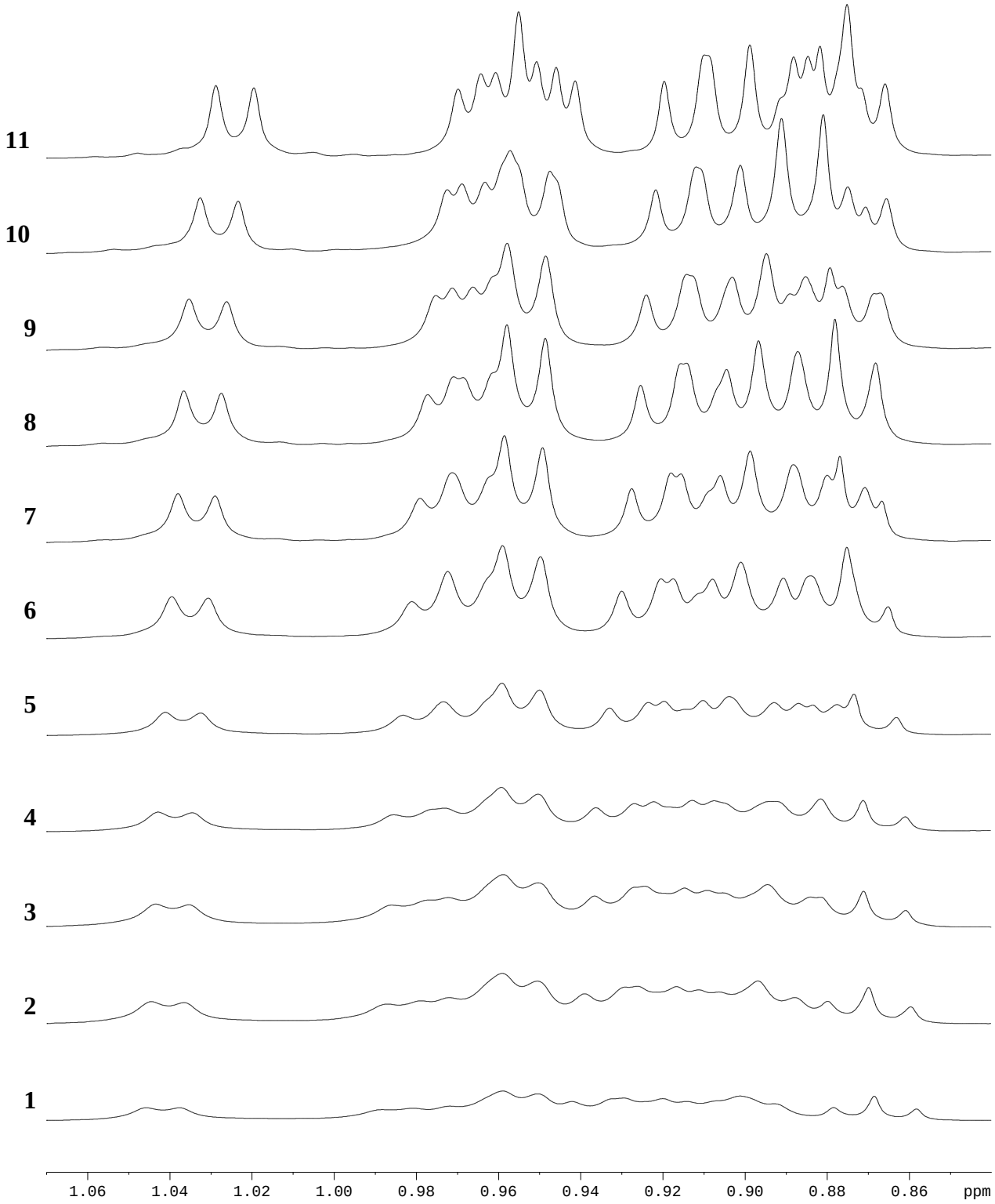
11
10
9
8
7
6
5
4
3
2
1
1.06
1.04
1.02
1.00
0.98
0.96
0.94
0.92
0.90
0.88
0.86
ppm

Stereo image of the solution structure

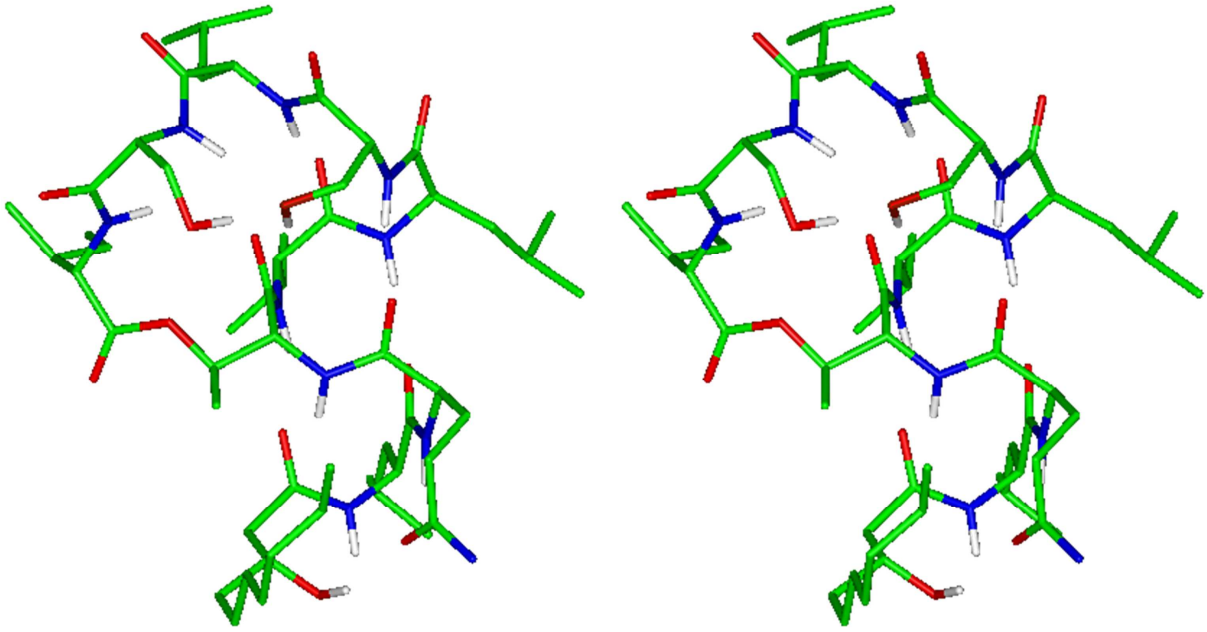

Solution structure statistics and restraint file

Statistics of the 40 lowest energy solution structures

Total distance restraints		127		
	intraresidual (|i-j|=0)	70		
	Interresidual (|i-j|=1)	35		
	long range (|i-j|>1)	22		
Violations [a]				
	Number >= 0.2 Å	11.25	±	1.81
	Sum of violations (Å)	5.48	±	0.52
	Maximum violation (Å)	0.52	±	0.05
Structure energy (kJ/mol) [a]				
	Total energy	-427.06	±	23.28
	bond energy	51.56	±	1.13
	Valence angle energy	219.77	±	6.85
	Torsion angle energy	-684.37	±	4.73
	Improper energy	-74.02	±	5.08
	Cross-term energy	1.84	±	0.39
	van der Waals energy	146.66	±	10.96
	Electrostatic energy	-88.50	±	23.10
Coordinate precision (Å) [b]				
	Heavy atoms (67)[c]	0.91	±	0.21
	Oligopeptide backbone (27)	0.15	±	0.08
	Helix backbone (15)[d]	0.10	±	0.04
	Ring backbone (22)	0.12	±	0.08

[a] Expressed as mean energy ± standard deviation
[b] Expressed as mean RMSD ± standard deviation; between brackets is the number of atoms
[c] All heavy atoms except for the HDA moiety
[d] All backbone atoms from Leu1 C' until Ser6 C^{α}

Restraint file

The restraint file used to obtain the solution structure is provided on pages 23-25, containing chirality, distance and dihedral restraints.

```
!BIOSYM restraint 1
!
#chiral
1:LEU_1:CA S
1:GLN_1B:CA R
1:THR_1C:CA R
1:THR_1C:CB R
1:VAL_1D:CA R
1:LEU_1E:CA R
1:SER_1F:CA R
1:LEU_1G:CA S
1:SER_1H:CA R
1:ILE_1I:CA S
1:ILE_1I:CB S
1:ALHD_1J:C2 R
!
#distance
1:ILE_1I:HN        1:ILE_1I:HA         0.000  3.167  10.00  10.00 1000.000
1:ILE_1I:HN        1:ILE_1I:HB         0.000  3.770  10.00  10.00 1000.000
1:ILE_1I:HN        1:ILE_1I:HG1*       0.000  3.583  10.00  10.00 1000.000
1:ILE_1I:HN        1:THR_1C:HA         0.000  4.044  10.00  10.00 1000.000
1:ILE_1I:HN        1:THR_1C:HB         0.000  4.933  10.00  10.00 1000.000
1:ILE_1I:HN        1:THR_1C:HG*        0.000  6.453  10.00  10.00 1000.000
1:ILE_1I:HN        1:VAL_1D:HA         0.000  3.958  10.00  10.00 1000.000
1:ILE_1I:HN        1:SER_1F:HG         0.000  4.697  10.00  10.00 1000.000
1:ILE_1I:HN        1:LEU_1G:HB1        0.000  3.699  10.00  10.00 1000.000
1:ILE_1I:HN        1:LEU_1G:HB2        0.000  3.356  10.00  10.00 1000.000
1:ILE_1I:HN        1:SER_1H:HN         0.000  2.469  10.00  10.00 1000.000
1:ILE_1I:HN        1:SER_1H:HA         0.000  3.520  10.00  10.00 1000.000
1:ILE_1I:HA        1:ILE_1I:HB         0.000  2.685  10.00  10.00 1000.000
1:ILE_1I:HA        1:ILE_1I:HG1*       0.000  4.447  10.00  10.00 1000.000
1:ILE_1I:HA        1:THR_1C:HG*        0.000  5.181  10.00  10.00 1000.000
1:ILE_1I:HB        1:ILE_1I:HG1*       0.000  3.656  10.00  10.00 1000.000
1:ILE_1I:HB        1:ILE_1I:HG2*       0.000  3.201  10.00  10.00 1000.000
1:ILE_1I:HD1*      1:ILE_1I:HN         0.000  5.041  10.00  10.00 1000.000
1:ILE_1I:HD1*      1:ILE_1I:HA         0.000  5.405  10.00  10.00 1000.000
1:ILE_1I:HD1*      1:ILE_1I:HB         0.000  3.875  10.00  10.00 1000.000
1:ILE_1I:HG1*      1:THR_1C:HB         0.000  3.902  10.00  10.00 1000.000
1:ILE_1I:HG1*      1:VAL_1D:HA         0.000  3.538  10.00  10.00 1000.000
1:ILE_1I:HG2*      1:ILE_1I:HN         0.000  4.202  10.00  10.00 1000.000
1:ILE_1I:HG2*      1:ILE_1I:HA         0.000  3.710  10.00  10.00 1000.000
1:LEU_1:HN         1:LEU_1:HA          0.000  2.536  10.00  10.00 1000.000
1:LEU_1:HN         1:GLN_1B:HN         0.000  3.240  10.00  10.00 1000.000
1:LEU_1:HN         1:ALHD_1J:HC*       0.000  3.421  10.00  10.00 1000.000
1:LEU_1:HN         1:ALHD_1J:H2        0.000  3.600  10.00  10.00 1000.000
1:LEU_1:HA         1:LEU_1:HD*         0.000  5.240  10.00  10.00 1000.000
1:LEU_1:HA         1:GLN_1B:HN         0.000  2.587  10.00  10.00 1000.000
1:LEU_1:HA         1:THR_1C:HN         0.000  4.562  10.00  10.00 1000.000
1:LEU_1:HB*        1:LEU_1:HA          0.000  3.472  10.00  10.00 1000.000
1:LEU_1:HB*        1:VAL_1D:HN         0.000  4.463  10.00  10.00 1000.000
1:LEU_1:HB*        1:VAL_1D:HB         0.000  3.477  10.00  10.00 1000.000
1:LEU_1:HB*        1:LEU_1:HD*         0.000  5.512  10.00  10.00 1000.000
1:LEU_1:HB*        1:GLN_1B:HN         0.000  5.074  10.00  10.00 1000.000
1:LEU_1:HD*        1:LEU_1:HN          0.000  5.710  10.00  10.00 1000.000
1:GLN_1B:HN        1:GLN_1B:HA         0.000  2.966  10.00  10.00 1000.000
1:GLN_1B:HN        1:GLN_1B:HB*        0.000  3.567  10.00  10.00 1000.000
1:GLN_1B:HN        1:GLN_1B:HG*        0.000  4.026  10.00  10.00 1000.000
1:GLN_1B:HN        1:THR_1C:HN         0.000  2.890  10.00  10.00 1000.000
1:GLN_1B:HA        1:GLN_1B:HB*        0.000  3.388  10.00  10.00 1000.000
1:GLN_1B:HB*       1:GLN_1B:HG*        0.000  4.301  10.00  10.00 1000.000
1:GLN_1B:HB*       1:THR_1C:HN         0.000  4.579  10.00  10.00 1000.000
```

```
1:GLN_1B:HG*       1:THR_1C:HN         0.000  4.216  10.00  10.00 1000.000
1:GLN_1B:HG*       1:GLN_1B:HA         0.000  3.950  10.00  10.00 1000.000
1:THR_1C:HN        1:THR_1C:HB         0.000  2.670  10.00  10.00 1000.000
1:THR_1C:HN        1:THR_1C:HG*        0.000  3.648  10.00  10.00 1000.000
1:THR_1C:HN        1:VAL_1D:HN         0.000  2.627  10.00  10.00 1000.000
1:THR_1C:HA        1:VAL_1D:HN         0.000  3.515  10.00  10.00 1000.000
1:THR_1C:HA        1:SER_1F:HG         0.000  2.606  10.00  10.00 1000.000
1:THR_1C:HA        1:SER_1H:HN         0.000  3.563  10.00  10.00 1000.000
1:THR_1C:HB        1:VAL_1D:HN         0.000  2.923  10.00  10.00 1000.000
1:THR_1C:HB        1:VAL_1D:HG1*       0.000  4.618  10.00  10.00 1000.000
1:THR_1C:HB        1:ALHD_1J:HC*       0.000  4.560  10.00  10.00 1000.000
1:THR_1C:HG*       1:THR_1C:HA         0.000  3.342  10.00  10.00 1000.000
1:THR_1C:HG*       1:VAL_1D:HN         0.000  5.780  10.00  10.00 1000.000
1:VAL_1D:HN        1:ILE_1I:HG1*       0.000  5.633  10.00  10.00 1000.000
1:VAL_1D:HN        1:VAL_1D:HA         0.000  3.063  10.00  10.00 1000.000
1:VAL_1D:HN        1:VAL_1D:HB         0.000  2.547  10.00  10.00 1000.000
1:VAL_1D:HN        1:LEU_1E:HN         0.000  2.762  10.00  10.00 1000.000
1:VAL_1D:HA        1:VAL_1D:HB         0.000  3.255  10.00  10.00 1000.000
1:VAL_1D:HA        1:LEU_1E:HN         0.000  3.933  10.00  10.00 1000.000
1:VAL_1D:HA        1:LEU_1G:HN         0.000  3.530  10.00  10.00 1000.000
1:VAL_1D:HA        1:LEU_1G:HB1        0.000  3.905  10.00  10.00 1000.000
1:VAL_1D:HA        1:SER_1H:HN         0.000  4.650  10.00  10.00 1000.000
1:VAL_1D:HB        1:LEU_1E:HN         0.000  2.834  10.00  10.00 1000.000
1:VAL_1D:HG2*      1:VAL_1D:HN         0.000  4.674  10.00  10.00 1000.000
1:VAL_1D:HG2*      1:VAL_1D:HA         0.000  3.722  10.00  10.00 1000.000
1:VAL_1D:HG1*      1:VAL_1D:HN         0.000  3.553  10.00  10.00 1000.000
1:VAL_1D:HG1*      1:VAL_1D:HA         0.000  3.566  10.00  10.00 1000.000
1:LEU_1E:HD*       1:LEU_1E:HN         0.000  6.274  10.00  10.00 1000.000
1:LEU_1E:HD*       1:LEU_1E:HA         0.000  4.762  10.00  10.00 1000.000
1:LEU_1E:HD*       1:LEU_1E:HB2        0.000  4.627  10.00  10.00 1000.000
1:LEU_1E:HD*       1:LEU_1E:HB1        0.000  4.774  10.00  10.00 1000.000
1:LEU_1E:HN        1:LEU_1E:HA         0.000  3.035  10.00  10.00 1000.000
1:LEU_1E:HN        1:LEU_1E:HG         0.000  2.626  10.00  10.00 1000.000
1:LEU_1E:HA        1:LEU_1E:HB2        0.000  2.899  10.00  10.00 1000.000
1:LEU_1E:HA        1:LEU_1E:HB1        0.000  2.591  10.00  10.00 1000.000
1:LEU_1E:HA        1:LEU_1E:HG         0.000  3.021  10.00  10.00 1000.000
1:LEU_1E:HA        1:SER_1F:HN         0.000  3.091  10.00  10.00 1000.000
1:LEU_1E:HB2       1:LEU_1E:HN         0.000  3.623  10.00  10.00 1000.000
1:LEU_1E:HB2       1:LEU_1E:HG         0.000  2.838  10.00  10.00 1000.000
1:LEU_1E:HB2       1:SER_1F:HN         0.000  3.425  10.00  10.00 1000.000
1:LEU_1E:HB1       1:SER_1F:HN         0.000  3.179  10.00  10.00 1000.000
1:SER_1F:HN        1:LEU_1E:HN         0.000  3.050  10.00  10.00 1000.000
1:SER_1F:HN        1:SER_1F:HB1        0.000  2.875  10.00  10.00 1000.000
1:SER_1F:HN        1:SER_1F:HB2        0.000  3.617  10.00  10.00 1000.000
1:SER_1F:HN        1:SER_1F:HG         0.000  2.522  10.00  10.00 1000.000
1:SER_1F:HN        1:SER_1H:HN         0.000  3.939  10.00  10.00 1000.000
1:SER_1F:HA        1:SER_1F:HB1        0.000  2.573  10.00  10.00 1000.000
1:SER_1F:HA        1:SER_1F:HB2        0.000  2.583  10.00  10.00 1000.000
1:SER_1F:HA        1:SER_1F:HG         0.000  4.053  10.00  10.00 1000.000
1:SER_1F:HB1       1:THR_1C:HG*        0.000  5.129  10.00  10.00 1000.000
1:SER_1F:HB1       1:SER_1F:HG         0.000  2.526  10.00  10.00 1000.000
1:SER_1F:HB2       1:SER_1F:HG         0.000  2.982  10.00  10.00 1000.000
1:SER_1F:HG        1:THR_1C:HG*        0.000  6.268  10.00  10.00 1000.000
1:SER_1F:HG        1:SER_1H:HN         0.000  3.381  10.00  10.00 1000.000
1:LEU_1G:HN        1:LEU_1E:HN         0.000  4.421  10.00  10.00 1000.000
1:LEU_1G:HN        1:LEU_1G:HA         0.000  3.150  10.00  10.00 1000.000
1:LEU_1G:HN        1:LEU_1G:HB1        0.000  3.435  10.00  10.00 1000.000
1:LEU_1G:HN        1:LEU_1G:HD*        0.000  6.457  10.00  10.00 1000.000
1:LEU_1G:HN        1:SER_1H:HN         0.000  2.786  10.00  10.00 1000.000
1:LEU_1G:HA        1:LEU_1G:HB1        0.000  2.800  10.00  10.00 1000.000
1:LEU_1G:HA        1:LEU_1G:HD*        0.000  4.861  10.00  10.00 1000.000
```

```
1:LEU_1G:HB1       1:LEU_1G:HD*        0.000  4.375  10.00  10.00 1000.000
1:LEU_1G:HB1       1:SER_1H:HN         0.000  3.942  10.00  10.00 1000.000
1:LEU_1G:HB2       1:SER_1H:HN         0.000  3.441  10.00  10.00 1000.000
1:LEU_1G:HD*       1:VAL_1D:HA         0.000  5.376  10.00  10.00 1000.000
1:ALHD_1J:HC*      1:ALHD_1J:H2        0.000  3.666  10.00  10.00 1000.000
1:ALHD_1J:H3*      1:LEU_1:HN          0.000  5.102  10.00  10.00 1000.000
1:ALHD_1J:H3*      1:ALHD_1J:HC*       0.000  4.510  10.00  10.00 1000.000
1:ALHD_1J:H3*      1:ALHD_1J:H2        0.000  3.652  10.00  10.00 1000.000
1:ALHD_1J:H4*      1:ALHD_1J:H2        0.000  3.924  10.00  10.00 1000.000
1:ALHD_1J:HH       1:LEU_1:HN          0.000  4.619  10.00  10.00 1000.000
1:ALHD_1J:HH       1:GLN_1B:HN         0.000  4.430  10.00  10.00 1000.000
1:SER_1H:HN        1:LEU_1G:HA         0.000  3.394  10.00  10.00 1000.000
1:SER_1H:HN        1:SER_1H:HA         0.000  3.126  10.00  10.00 1000.000
1:SER_1H:HN        1:SER_1H:HB2        0.000  3.264  10.00  10.00 1000.000
1:SER_1H:HA        1:SER_1H:HB2        0.000  2.598  10.00  10.00 1000.000
1:SER_1H:HA        1:SER_1H:HB1        0.000  2.771  10.00  10.00 1000.000
1:SER_1H:HA        1:SER_1H:HG         0.000  3.495  10.00  10.00 1000.000
1:SER_1H:HB1       1:ILE_1I:HN         0.000  3.725  10.00  10.00 1000.000
1:SER_1H:HB1       1:SER_1H:HN         0.000  2.972  10.00  10.00 1000.000
1:SER_1H:HG        1:ILE_1I:HN         0.000  3.989  10.00  10.00 1000.000
1:SER_1H:HG        1:SER_1H:HN         0.000  2.741  10.00  10.00 1000.000
1:SER_1H:HG        1:SER_1H:HB2        0.000  2.341  10.00  10.00 1000.000
!
#NMR_dihedral
1:ALHD_1J:C    1:ALHD_1J:C1    1:LEU_1:N      1:LEU_1:CA    175 -175 100 100 1000
1:LEU_1:CA     1:LEU_1:C       1:GLN_1B:N     1:GLN_1B:CA   175 -175 100 100 1000
1:GLN_1B:CA    1:GLN_1B:C      1:THR_1C:N     1:THR_1C:CA   175 -175 100 100 1000
1:THR_1C:CA    1:THR_1C:C      1:VAL_1D:N     1:VAL_1D:CA   175 -175 100 100 1000
1:VAL_1D:CA    1:VAL_1D:C      1:LEU_1E:N     1:LEU_1E:CA   175 -175 100 100 1000
1:LEU_1E:CA    1:LEU_1E:C      1:SER_1F:N     1:SER_1F:CA   175 -175 100 100 1000
1:SER_1F:CA    1:SER_1F:C      1:LEU_1G:N     1:LEU_1G:CA   175 -175 100 100 1000
1:LEU_1G:CA    1:LEU_1G:C      1:SER_1H:N     1:SER_1H:CA   175 -175 100 100 1000
1:SER_1H:CA    1:SER_1H:C      1:ILE_1I:N     1:ILE_1I:CA   175 -175 100 100 1000
```

$^{1}H/^{2}H$ exchange curves in acetonitrile

The moment of adding the D_2O is chosen as 0 s, while the peak integrals are normalised to the first data point measured.

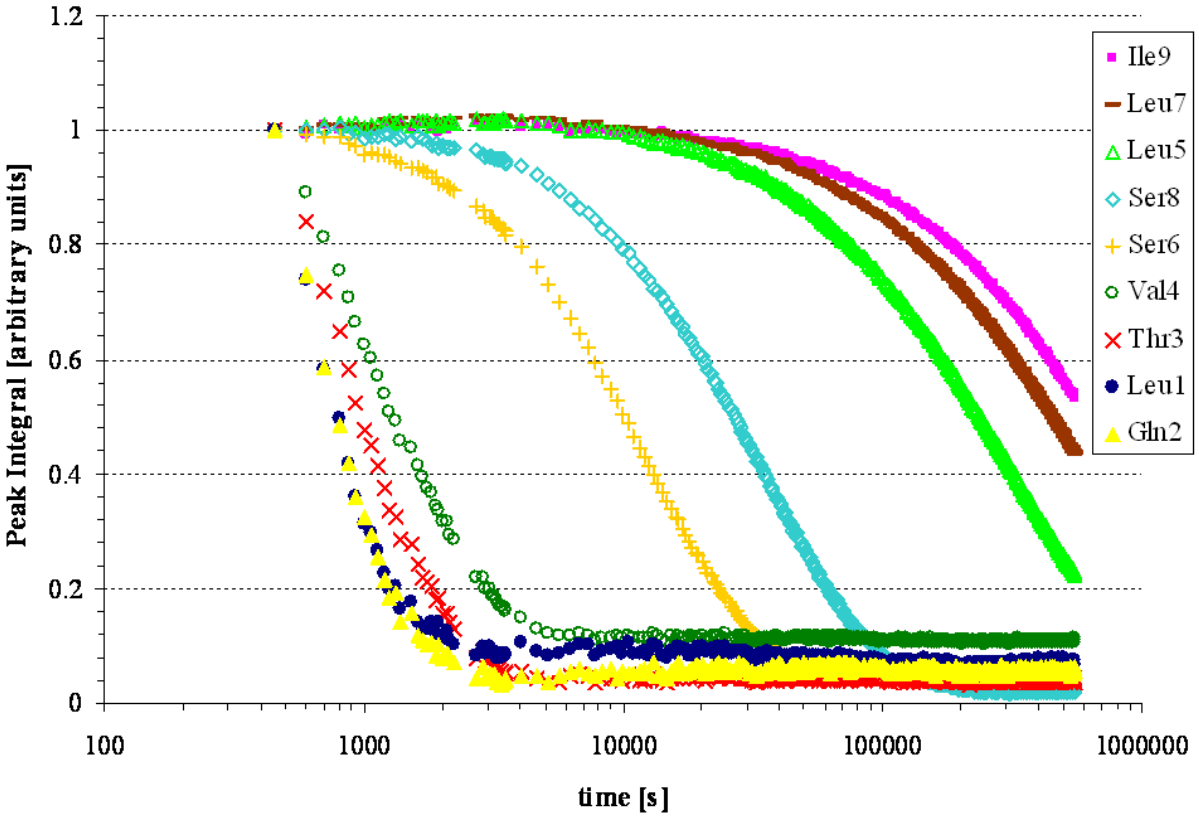

Magnetic field dependence of the pseudodesmin A resonance line widths in DMSO solution

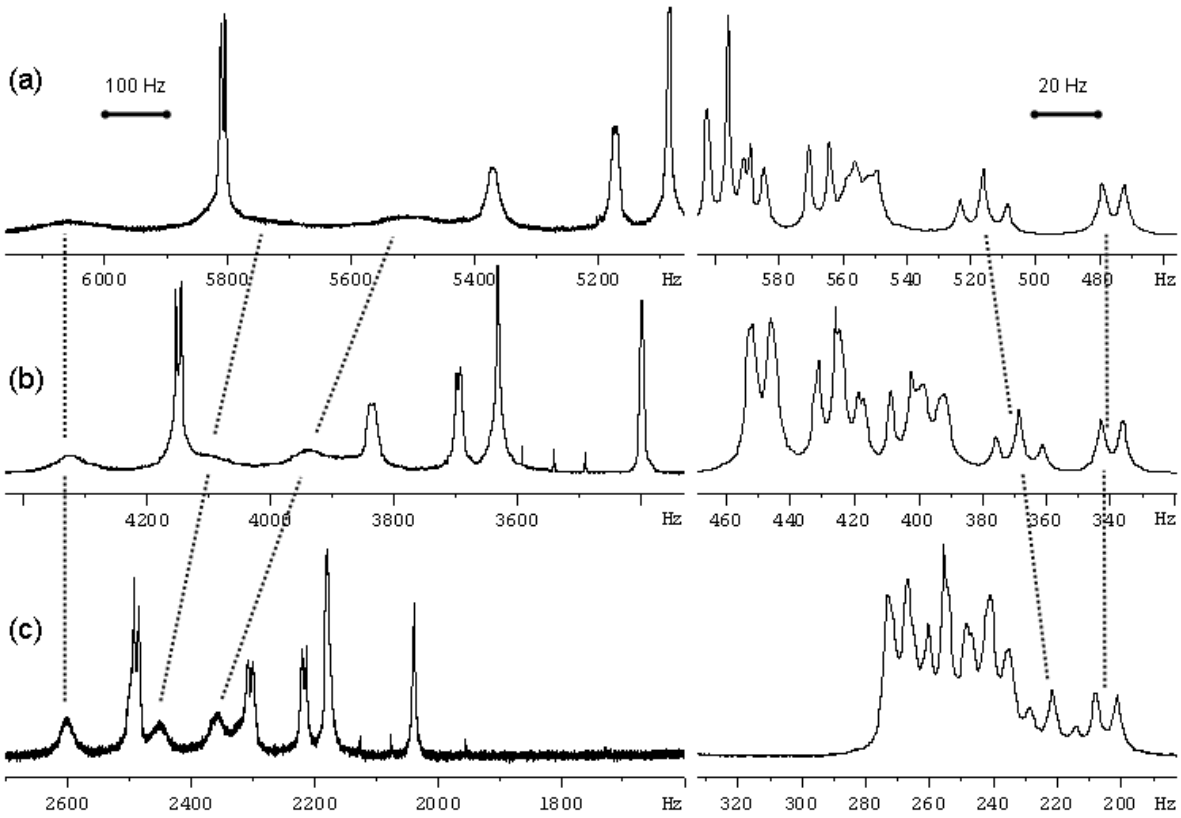

(a) 700.13 MHz
(b) 500.13 MHz
(c) 300.13 MHz

The H^N region (left) and methyl region (right) of the 1D ^1H NMR spectrum of pseudodesmin A in DMSO solution is shown at three different field strengths on a hertz scale. Note the increase in line width for several H^N resonances with increasing line width, indicating an exchange process going towards the point of coalescence. For comparison, the methyl region shows no change in line width.

Spectra were recorded on a 16.4 T Bruker Avance II spectrometer equipped with a 5mm $^1H,^{13}C,^{15}N$ TXI-Z probe, a 11.7 T Bruker DRX spectrometer equipped with a 5mm $^1H,^{13}C,^{15}N$ TXI-Z probe and a 7.0 T Bruker Avance spectrometer equipped with a 5mm BBO gradient probe. Temperature was set at 298.0 K on each spectrometer.

Temperature dependence of the pseudodesmin A resonance line widths and temperature coefficients of amide ^{1}H resonances in DMSO solution

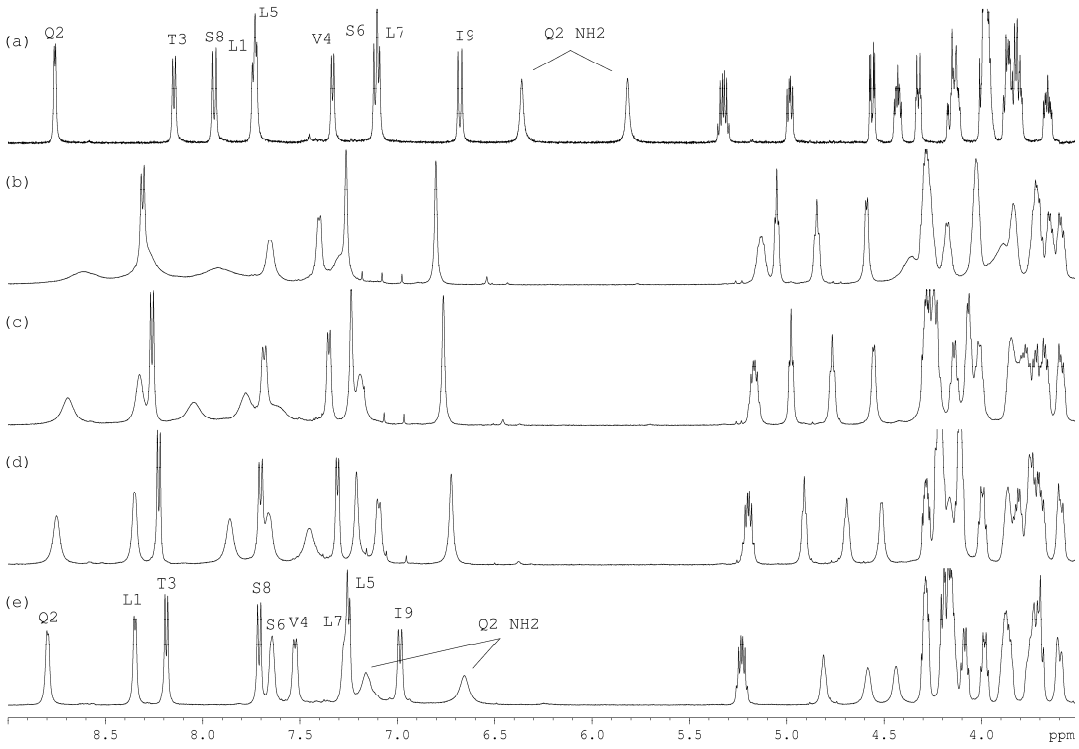

H^N and H^α regions of the 500.13 MHz ^{1}H NMR spectrum of pseudodesmin A in (a) acetonitrile at 298.0 K; (b) DMSO at 297.4 K; (c) DMSO at 309.4 K; (d) DMSO 321.4 K; (e) DMSO at 339.4 K. Amide H^N resonances are labelled according to residue.

Amide temperature coefficients in DMSO [ppb/K]		
Leu1	1.27	(0.72)[a]
Gln2	4.43	(0.95)[b]
Thr3	-2.88	(0.98)
Val4	-9.48	(0.99)
Leu5	-3.61	(1.00)
Ser6	-14.07	(0.99)
Leu7	-11.93	(0.99)
Ser8	1.34	(0.89)[c]
Ile9	-7.39	(0.99)
Gln2 NH_2 1	-2.41	(1.00)
Gln2 NH_2 2	-3.47	(1.00)

Listed values are the slopes obtained from linear regression between chemical shift and temperature, expressed in ppb/K. The numbers in brackets are Pearson correlation coefficients (R^2).

[a] Non-linear behaviour, parabolic fit (R^2 = 1.00): $\delta[ppm] = -7.67\times10^{-5}T^2 + 5.06\times10^{-2}T + 0.016$

[b] Non-linear behaviour, parabolic fit (R^2 = 1.00): $\delta[ppm] = -8.02\times10^{-5}T^2 + 5.59\times10^{-2}T - 0.800$

[c] Non-linear behaviour, parabolic fit (R^2 = 1.00): $\delta[ppm] = -3.90\times10^{-5}T^2 + 2.62\times10^{-2}T + 3.317$

```
REMARK pseudodesminA_solstruc.pdb
REMARK The lowest energy NMR solution structure of pseudodesmin A in PDB format

REMARK   4
REMARK   4 KMCP COMPLIES WITH FORMAT V. 2.0,  8-NOV-2007
ATOM      1  N   LEU     1       0.058  21.889  -0.337  1.00  0.00           N
ATOM      2  CA  LEU     1       1.273  22.713  -0.365  1.00  0.00           C
ATOM      3  C   LEU     1       1.449  23.364   1.053  1.00  0.00           C
ATOM      4  O   LEU     1       1.508  24.587   1.186  1.00  0.00           O
ATOM      5  CB  LEU     1       1.279  23.765  -1.496  1.00  0.00           C
ATOM      6  CG  LEU     1       1.153  23.247  -2.949  1.00  0.00           C
ATOM      7  CD1 LEU     1       1.084  24.440  -3.921  1.00  0.00           C
ATOM      8  CD2 LEU     1       2.293  22.296  -3.357  1.00  0.00           C
ATOM      9  H   LEU     1       0.131  20.910  -0.584  1.00  0.00           H
ATOM     10  HA  LEU     1       2.127  22.027  -0.499  1.00  0.00           H
ATOM     11 1HB  LEU     1       0.467  24.489  -1.309  1.00  0.00           H
ATOM     12 2HB  LEU     1       2.225  24.331  -1.402  1.00  0.00           H
ATOM     13  HG  LEU     1       0.200  22.692  -3.041  1.00  0.00           H
ATOM     14 2HD1 LEU     1       2.011  25.035  -3.878  1.00  0.00           H
ATOM     15 3HD1 LEU     1       0.949  24.107  -4.964  1.00  0.00           H
ATOM     16 1HD1 LEU     1       0.243  25.111  -3.679  1.00  0.00           H
ATOM     17 2HD2 LEU     1       3.272  22.794  -3.267  1.00  0.00           H
ATOM     18 3HD2 LEU     1       2.320  21.386  -2.737  1.00  0.00           H
ATOM     19 1HD2 LEU     1       2.178  21.973  -4.405  1.00  0.00           H
ATOM     20  N   GLN     1B      1.575  22.505   2.140  1.00  0.00           N
ATOM     21  CA  GLN     1B      1.782  23.074   3.479  1.00  0.00           C
ATOM     22  C   GLN     1B      0.536  23.902   3.937  1.00  0.00           C
ATOM     23  O   GLN     1B      0.718  24.811   4.746  1.00  0.00           O
ATOM     24  CB  GLN     1B      2.128  22.042   4.577  1.00  0.00           C
ATOM     25  CG  GLN     1B      1.103  20.926   4.901  1.00  0.00           C
ATOM     26  CD  GLN     1B      1.211  19.762   3.926  1.00  0.00           C
ATOM     27  OE1 GLN     1B      0.713  19.797   2.807  1.00  0.00           O
ATOM     28  NE2 GLN     1B      1.911  18.668   4.382  1.00  0.00           N
ATOM     29  H   GLN     1B      1.460  21.502   2.049  1.00  0.00           H
ATOM     30  HA  GLN     1B      2.612  23.796   3.419  1.00  0.00           H
ATOM     31 1HB  GLN     1B      3.101  21.576   4.343  1.00  0.00           H
ATOM     32 2HB  GLN     1B      2.290  22.634   5.497  1.00  0.00           H
ATOM     33 1HG  GLN     1B      1.265  20.575   5.935  1.00  0.00           H
ATOM     34 2HG  GLN     1B      0.067  21.298   4.858  1.00  0.00           H
ATOM     35 1HE2 GLN     1B      2.320  18.646   5.299  1.00  0.00           H
ATOM     36 2HE2 GLN     1B      2.002  17.880   3.763  1.00  0.00           H
ATOM     37  N   THR     1C     -0.744  23.647   3.448  1.00  0.00           N
ATOM     38  CA  THR     1C     -1.871  24.501   3.858  1.00  0.00           C
ATOM     39  C   THR     1C     -1.772  25.893   3.178  1.00  0.00           C
ATOM     40  O   THR     1C     -2.048  26.891   3.845  1.00  0.00           O
ATOM     41  CB  THR     1C     -3.287  23.936   3.590  1.00  0.00           C
ATOM     42  CG2 THR     1C     -3.476  22.676   4.452  1.00  0.00           C
ATOM     43  H   THR     1C     -0.874  23.014   2.672  1.00  0.00           H
ATOM     44  HA  THR     1C     -1.778  24.693   4.933  1.00  0.00           H
ATOM     45  HB  THR     1C     -3.396  23.741   2.509  1.00  0.00           H
ATOM     46 1HG2 THR     1C     -4.474  22.234   4.331  1.00  0.00           H
ATOM     47 2HG2 THR     1C     -2.720  21.908   4.230  1.00  0.00           H
ATOM     48 3HG2 THR     1C     -3.359  22.956   5.516  1.00  0.00           H
ATOM     49  N   VAL     1D     -1.378  25.992   1.859  1.00  0.00           N
ATOM     50  CA  VAL     1D     -1.176  27.320   1.265  1.00  0.00           C
ATOM     51  C   VAL     1D      0.001  28.008   2.038  1.00  0.00           C
ATOM     52  O   VAL     1D     -0.144  29.173   2.400  1.00  0.00           O
ATOM     53  CB  VAL     1D     -0.872  27.288  -0.247  1.00  0.00           C
ATOM     54  CG1 VAL     1D     -2.002  26.607  -1.051  1.00  0.00           C
ATOM     55  CG2 VAL     1D     -0.599  28.684  -0.840  1.00  0.00           C
ATOM     56  H   VAL     1D     -1.154  25.163   1.316  1.00  0.00           H
```

```
ATOM     57  HA  VAL     1D     -2.071  27.929   1.473  1.00  0.00           H
ATOM     58  HB  VAL     1D      0.045  26.686  -0.384  1.00  0.00           H
ATOM     59 1HG1 VAL     1D     -2.210  25.580  -0.711  1.00  0.00           H
ATOM     60 2HG1 VAL     1D     -2.943  27.171  -0.962  1.00  0.00           H
ATOM     61 3HG1 VAL     1D     -1.746  26.544  -2.121  1.00  0.00           H
ATOM     62 2HG2 VAL     1D      0.264  29.179  -0.366  1.00  0.00           H
ATOM     63 3HG2 VAL     1D     -0.384  28.618  -1.919  1.00  0.00           H
ATOM     64 1HG2 VAL     1D     -1.473  29.344  -0.712  1.00  0.00           H
ATOM     65  N   LEU     1E      1.159  27.296   2.351  1.00  0.00           N
ATOM     66  CA  LEU     1E      2.232  27.938   3.136  1.00  0.00           C
ATOM     67  C   LEU     1E      1.696  28.468   4.505  1.00  0.00           C
ATOM     68  O   LEU     1E      2.016  29.583   4.911  1.00  0.00           O
ATOM     69  CB  LEU     1E      3.410  26.997   3.437  1.00  0.00           C
ATOM     70  CG  LEU     1E      4.328  26.642   2.244  1.00  0.00           C
ATOM     71  CD1 LEU     1E      5.064  27.865   1.668  1.00  0.00           C
ATOM     72  CD2 LEU     1E      5.346  25.562   2.654  1.00  0.00           C
ATOM     73  H   LEU     1E      1.282  26.337   2.034  1.00  0.00           H
ATOM     74  HA  LEU     1E      2.572  28.819   2.605  1.00  0.00           H
ATOM     75 1HB  LEU     1E      4.003  27.478   4.234  1.00  0.00           H
ATOM     76 2HB  LEU     1E      3.010  26.076   3.885  1.00  0.00           H
ATOM     77  HG  LEU     1E      3.701  26.222   1.436  1.00  0.00           H
ATOM     78 2HD1 LEU     1E      4.371  28.623   1.270  1.00  0.00           H
ATOM     79 3HD1 LEU     1E      5.686  28.350   2.438  1.00  0.00           H
ATOM     80 1HD1 LEU     1E      5.729  27.569   0.840  1.00  0.00           H
ATOM     81 2HD2 LEU     1E      5.986  25.268   1.805  1.00  0.00           H
ATOM     82 3HD2 LEU     1E      6.005  25.932   3.457  1.00  0.00           H
ATOM     83 1HD2 LEU     1E      4.849  24.650   3.022  1.00  0.00           H
ATOM     84  N   SER     1F      0.893  27.616   5.232  1.00  0.00           N
ATOM     85  CA  SER     1F      0.358  27.935   6.561  1.00  0.00           C
ATOM     86  C   SER     1F     -0.634  29.151   6.519  1.00  0.00           C
ATOM     87  O   SER     1F     -0.892  29.746   7.565  1.00  0.00           O
ATOM     88  CB  SER     1F     -0.475  26.769   7.138  1.00  0.00           C
ATOM     89  OG  SER     1F     -1.751  26.606   6.523  1.00  0.00           O
ATOM     90  H   SER     1F      0.758  26.695   4.838  1.00  0.00           H
ATOM     91  HA  SER     1F      1.182  28.191   7.244  1.00  0.00           H
ATOM     92 1HB  SER     1F      0.064  25.805   7.081  1.00  0.00           H
ATOM     93 2HB  SER     1F     -0.672  26.972   8.199  1.00  0.00           H
ATOM     94  HG  SER     1F     -1.554  26.533   5.566  1.00  0.00           H
ATOM     95  N   LEU     1G     -1.283  29.487   5.330  1.00  0.00           N
ATOM     96  CA  LEU     1G     -2.321  30.521   5.280  1.00  0.00           C
ATOM     97  C   LEU     1G     -3.586  30.046   6.080  1.00  0.00           C
ATOM     98  O   LEU     1G     -4.420  30.878   6.436  1.00  0.00           O
ATOM     99  CB  LEU     1G     -2.817  30.826   3.836  1.00  0.00           C
ATOM    100  CG  LEU     1G     -2.542  32.258   3.324  1.00  0.00           C
ATOM    101  CD1 LEU     1G     -1.039  32.579   3.232  1.00  0.00           C
ATOM    102  CD2 LEU     1G     -3.214  32.472   1.956  1.00  0.00           C
ATOM    103  H   LEU     1G     -0.966  29.090   4.451  1.00  0.00           H
ATOM    104  HA  LEU     1G     -1.960  31.423   5.781  1.00  0.00           H
ATOM    105 1HB  LEU     1G     -2.395  30.110   3.116  1.00  0.00           H
ATOM    106 2HB  LEU     1G     -3.905  30.632   3.793  1.00  0.00           H
ATOM    107  HG  LEU     1G     -2.999  32.969   4.039  1.00  0.00           H
ATOM    108 2HD1 LEU     1G     -0.876  33.615   2.893  1.00  0.00           H
ATOM    109 3HD1 LEU     1G     -0.525  32.466   4.200  1.00  0.00           H
ATOM    110 1HD1 LEU     1G     -0.538  31.911   2.512  1.00  0.00           H
ATOM    111 2HD2 LEU     1G     -4.301  32.293   2.004  1.00  0.00           H
ATOM    112 3HD2 LEU     1G     -3.064  33.500   1.588  1.00  0.00           H
ATOM    113 1HD2 LEU     1G     -2.794  31.783   1.204  1.00  0.00           H
ATOM    114  C1  ALHD    1J     -1.187  22.322   0.068  1.00  0.00           C
ATOM    115  O2  ALHD    1J     -1.382  23.451   0.506  1.00  0.00           O
ATOM    116  C   ALHD    1J     -2.342  21.314  -0.012  1.00  0.00           C
ATOM    117  C2  ALHD    1J     -2.132  20.221   1.044  1.00  0.00           C
```

```
ATOM    118  C3  ALHD    1J     -3.381  19.339   1.238  1.00  0.00           C
ATOM    119  C4  ALHD    1J     -3.276  18.269   2.347  1.00  0.00           C
ATOM    120  C5  ALHD    1J     -3.112  18.842   3.767  1.00  0.00           C
ATOM    121  C6  ALHD    1J     -3.031  17.763   4.861  1.00  0.00           C
ATOM    122  C7  ALHD    1J     -2.964  18.312   6.301  1.00  0.00           C
ATOM    123  C8  ALHD    1J     -1.731  19.181   6.614  1.00  0.00           C
ATOM    124  C9  ALHD    1J     -1.683  19.646   8.075  1.00  0.00           C
ATOM    125  OH  ALHD    1J     -1.000  19.439   0.659  1.00  0.00           O
ATOM    126 1HC  ALHD    1J     -2.403  20.869  -1.019  1.00  0.00           H
ATOM    127 2HC  ALHD    1J     -3.275  21.869   0.164  1.00  0.00           H
ATOM    128  H2  ALHD    1J     -1.907  20.740   1.994  1.00  0.00           H
ATOM    129 1H3  ALHD    1J     -3.599  18.836   0.277  1.00  0.00           H
ATOM    130 2H3  ALHD    1J     -4.252  19.985   1.451  1.00  0.00           H
ATOM    131 1H4  ALHD    1J     -2.435  17.588   2.126  1.00  0.00           H
ATOM    132 2H4  ALHD    1J     -4.188  17.645   2.319  1.00  0.00           H
ATOM    133 1H5  ALHD    1J     -3.960  19.516   3.983  1.00  0.00           H
ATOM    134 2H5  ALHD    1J     -2.200  19.462   3.809  1.00  0.00           H
ATOM    135 1H6  ALHD    1J     -2.150  17.122   4.675  1.00  0.00           H
ATOM    136 2H6  ALHD    1J     -3.913  17.101   4.779  1.00  0.00           H
ATOM    137 1H7  ALHD    1J     -2.984  17.460   7.005  1.00  0.00           H
ATOM    138 2H7  ALHD    1J     -3.879  18.898   6.506  1.00  0.00           H
ATOM    139 1H8  ALHD    1J     -1.727  20.070   5.961  1.00  0.00           H
ATOM    140 2H8  ALHD    1J     -0.813  18.614   6.381  1.00  0.00           H
ATOM    141 1H9  ALHD    1J     -1.649  18.787   8.764  1.00  0.00           H
ATOM    142 2H9  ALHD    1J     -0.794  20.268   8.268  1.00  0.00           H
ATOM    143 3H9  ALHD    1J     -2.573  20.246   8.326  1.00  0.00           H
ATOM    144  HH  ALHD    1J     -0.546  19.203   1.487  1.00  0.00           H
ATOM    145  N   SER     1H     -3.786  28.689   6.283  1.00  0.00           N
ATOM    146  CA  SER     1H     -4.972  28.136   6.985  1.00  0.00           C
ATOM    147  C   SER     1H     -5.983  27.469   6.002  1.00  0.00           C
ATOM    148  O   SER     1H     -7.144  27.234   6.330  1.00  0.00           O
ATOM    149  CB  SER     1H     -4.554  27.085   8.011  1.00  0.00           C
ATOM    150  OG  SER     1H     -4.097  25.836   7.518  1.00  0.00           O
ATOM    151  H   SER     1H     -2.983  28.075   6.166  1.00  0.00           H
ATOM    152  HA  SER     1H     -5.482  28.948   7.511  1.00  0.00           H
ATOM    153 1HB  SER     1H     -3.786  27.533   8.656  1.00  0.00           H
ATOM    154 2HB  SER     1H     -5.411  26.844   8.622  1.00  0.00           H
ATOM    155  HG  SER     1H     -3.180  26.031   7.266  1.00  0.00           H
ATOM    156  N   ILE     1I     -5.477  27.123   4.770  1.00  0.00           N
ATOM    157  CA  ILE     1I     -6.163  26.377   3.703  1.00  0.00           C
ATOM    158  C   ILE     1I     -5.424  25.053   3.325  1.00  0.00           C
ATOM    159  O   ILE     1I     -5.852  24.231   2.525  1.00  0.00           O
ATOM    160  CB  ILE     1I     -6.388  27.232   2.428  1.00  0.00           C
ATOM    161  CG1 ILE     1I     -5.058  27.681   1.766  1.00  0.00           C
ATOM    162  CG2 ILE     1I     -7.328  28.421   2.732  1.00  0.00           C
ATOM    163  CD1 ILE     1I     -5.212  28.493   0.472  1.00  0.00           C
ATOM    164  H   ILE     1I     -4.523  27.404   4.601  1.00  0.00           H
ATOM    165  HA  ILE     1I     -7.132  26.036   4.100  1.00  0.00           H
ATOM    166  HB  ILE     1I     -6.915  26.570   1.716  1.00  0.00           H
ATOM    167 1HG1 ILE     1I     -4.471  28.282   2.483  1.00  0.00           H
ATOM    168 2HG1 ILE     1I     -4.443  26.788   1.543  1.00  0.00           H
ATOM    169 2HG2 ILE     1I     -7.651  28.938   1.814  1.00  0.00           H
ATOM    170 3HG2 ILE     1I     -8.241  28.082   3.249  1.00  0.00           H
ATOM    171 1HG2 ILE     1I     -6.837  29.166   3.380  1.00  0.00           H
ATOM    172 2HD1 ILE     1I     -4.226  28.762   0.061  1.00  0.00           H
ATOM    173 3HD1 ILE     1I     -5.755  27.921  -0.297  1.00  0.00           H
ATOM    174 1HD1 ILE     1I     -5.757  29.435   0.643  1.00  0.00           H
ATOM    175  OH  OHH     1K     -4.243  24.928   3.987  1.00  0.00           O
END
```